Title: **Cis-regulatory evolution of *Wnt*-family genes contributes to a morphological difference between silkworm species.**

Authors: Kenta Tomihara[1,†], Ana Pinharanda[2,3,4†], Young Mi Kwon[2], Andrew M. Taverner[5], Laura Kors[6], Matthew L. Aardema[7], Julia C. Holder[2], Lin Poyraz[2], Patrick F. Reilly[5], Takashi Kiuchi[1,*], and Peter Andolfatto[2,*]

Affiliations:

[1]Department of Agricultural and Environmental Biology, Graduate School of Agricultural and Life Sciences, University of Tokyo; Yayoi 1-1-1, Bunkyo-ku, Tokyo 113-8657, Japan.

[2]Department of Biological Sciences, Columbia University; 1212 Amsterdam Avenue, New York, NY, 10027, USA.

[3]Department of Immunology and Infectious Diseases, Harvard T.H. Chan School of Public Health; Boston, MA, 02115, USA.

[4]Infectious Disease and Microbiome Program, Broad Institute of MIT and Harvard; Cambridge, MA, 02142, USA.

[5]Lewis-Sigler Institute for Integrative Genomics, Princeton University; Princeton, NJ, 08544, USA.

[6]Department of Biology, Barnard College, Columbia University; New York, NY 10027, USA

[7]Department of Biology, Montclair State University; Montclair, NJ, 07043, USA

[†]Contributed equally to this work

*Co-supervised this work.

Corresponding authors. Email: pa2543@columbia.edu, kiuchi@g.ecc.u-tokyo.ac.jp

Abstract

Closely related species often exhibit distinct morphologies that can contribute to species-specific adaptations and reproductive isolation. One example are Lepidopteran caterpillar appendages, such as the "caudal horn" of Bombycoidea moths, which have evolved substantial morphological diversity among species in this group. Using interspecific crosses, we identify the genetic basis of the caudal horn size difference between *Bombyx mori* and its closest relative *B. mandarina*. One major QTL contributes more than 10% to the mean horn length difference between the two species. This QTL encompasses a conserved *Wnt*-family gene cluster, key upstream regulators that are well-known for their roles in morphological diversification in animals. Using allele-specific expression analysis and CRISPR/Cas9 knockouts, we show that cis-regulatory changes to *Wnt1* and *Wnt6* contribute to the species difference in caudal horn size. This kind of modularity enables highly pleiotropic genes, including key upstream growth regulators, to contribute to the evolution of morphological traits without causing widespread deleterious effects.

Significance

This study explores the genetic basis of a distinct morphological trait that varies between two closely related moth species, providing insights into the evolution of morphological diversity. By identifying cis-regulatory changes in two *Wnt*-family genes as major contributors, this work underscores the importance of developmental gene regulatory networks in shaping species-specific traits. The findings illustrate how even small modifications in major upstream regulator genes can drive significant phenotypic variation, revealing how genetic changes in key growth regulators fuel the diversification of form and function. These results advance our understanding of the mechanisms behind the evolution of complex morphological traits.

One-Sentence Summary: Cis-regulatory evolution of *Wnt* genes is a major contributor to species-specific morphology in moth caterpillars.

Main Text:

Introduction

Understanding the genetic mechanisms underlying morphological evolution has long been a central goal in evolutionary biology (1–3). This pursuit has yielded a growing number of cases in which the genetic basis of morphological traits that differentiate populations and species has been identified (4). However, it is increasingly clear that the genetic architecture of morphological evolution is both complex and varied. In some cases, dramatic phenotypic changes can be attributed to a few loci of large effect; in others, they involve many genes of smaller effect. Ongoing debates center on whether evolutionary shifts are typically driven by changes in high-level regulatory genes or their downstream targets, and on the relative importance of regulatory versus protein-coding sequence changes. Resolving these questions remains essential for a comprehensive understanding of the genetic basis of morphological change (5–7).

Insects have evolved a wide range of morphological adaptations, including projections used for combat (8), mate choice (9), digging (10), sensing (11), and defense (12). Among these, lepidopteran caterpillars exhibit an impressive range of protruding structures, such as setae, spines and horns. The evolution of these structures across different species has resulted in remarkably diverse caterpillar morphologies (**Fig 1**). One notable example is the "caudal horn", a conspicuous fleshy projection found at the posterior end of Bombycoidea caterpillars (**Fig 1B**). The caudal horn exhibits substantial variation in size, shape and color among different species in the family, suggesting potential adaptive importance of this structure. Little is known about its function, but it has been speculated that in some species it may play a role in crypsis or in sensory capacity (13). Specifically, some Bombycidae have been reported to move their caudal horn when disturbed (14). While for other Lepidoptera, caterpillars with horn-like projections rapidly beat them when approached by parasitoids, suggesting a potential role for such horns in defense (15).

The mechanisms underlying evolutionary gains and losses of morphological innovations, like the caudal horn, are often inaccessible to genetic analysis due to reproductive barriers between species exhibiting different traits. In this study, we take advantage of the fact that the domesticated silkworm *Bombyx mori* and its closest relative *B. mandarina* (both members of the Bombycoidea group, **Fig 1**) produce fertile hybrids. *B. mori* is believed to have been domesticated ~4-10 thousand years ago (16–18) from a *B. mandarina*-like ancestor that may have started diverging from extant *B. mandarina* lineages more than 1 million generations ago (see *Divergence dating*(19). During this time, *B. mori* and *B. mandarina* have diverged in a variety of morphological, physiological and behavioral traits. Several of these traits, including size, loss of flight, silk yield and larval foraging behavior are likely to be directly associated with the domestication (20–22). However, for other traits – such as larval caudal horn length, olfactory capacity, and pigmentation – their adaptive significance remains unclear, although in the case of pigmentation, darker coloration in *B. mandarina* may contribute to crypsis, while its reduction in *B. mori* might facilitate detection by farmers ((23–25); **Fig 1B**, **Fig S1**).

Given the broad diversity in larval appendages among Lepidoptera, of which diversification of the caudal horn among the Bombicoidea is a part, we use interspecific crosses and advances in high-throughput genotyping to investigate the genetic basis of the caudal horn length difference between *B. mori* and *B. mandarina*. Further, using gene expression studies and targeted knock-outs, we identify causative loci underlying the largest QTL contributing to the caudal horn length difference between species. Our work sheds light on how novel species-specific morphological traits can evolve over relatively short evolutionary timescales.

Results

Multiple QTL underlie caudal horn length divergence. The caudal horn of *B. mandarina* Sakado strain (3.51 ± 0.08 mm) is over 3-fold longer than that of *B. mori* p50T strain (0.94 ± 0.11 mm) (**Fig 2A**). This length difference is consistent across seven additional *B. mori* strains (**Fig S1A**). The mean caudal horn length for p50T/Sakado F1 hybrids is intermediate (2.28 ± 0.09 mm) suggesting that some alleles contributing to longer caudal horn length in *B. mandarina* are partially dominant. Within species, body size and caudal horn size exhibit positive allometry, as often observed for morphological traits. In contrast, the opposite pattern is observed between species, with *B. mori* caterpillars having a shorter horn than *B. mandarina*, despite the former being substantially larger (22) (**Fig S1D**). To investigate the genetic basis of caudal horn length divergence between species, we generated two hybrid mapping populations (694 BC1 progeny and 327 F2 progeny, **Fig S2**). The phenotype distribution of BC1 progeny continuously spans the range of phenotypes between *B. mori* p50T and p50T/Sakado F1 hybrids (**Fig 2A**), as expected for trait variation that is encoded by several causative loci. The broad distribution of BC1 phenotypes also implies that at least some large-effect loci are likely to contribute to the trait difference between species.

Quantitative trait locus (QTL) analyses of these two mapping populations reveal multiple loci contributing to caudal horn length divergence between species. Analysis of BC1 mapping population identifies eight QTL with significant effects on caudal horn length (**Fig 2B**). The largest effect QTL is localized to a 600 kilobase interval on chromosome 4 (Chr4). This QTL accounts for 18% of the variance among BC1 progeny and 11% of the mean length difference between species (**Table S1**, **Fig 2C**). The three largest effect BC1 QTL (Chr4, Chr5 and Chr21) jointly account for 27% of the difference in mean length between species. The remaining QTL have smaller, marginally significant effects and are less well spatially resolved (**Fig 2C**, **Table S1**). Caterpillar weight (a proxy for size) and sex also contribute significantly to the variance in caudal horn length among BC1 progeny. Interestingly, all eight QTL have effects in the same direction, *i.e.* the *B. mandarina* allele is associated with longer mean caudal horn length (QTL Sign Test p-value =0.008; **Fig 2C**, **Fig S3**). The biased direction of QTL effects implies that difference in caudal horn size between species is not likely to be solely attributable to genetic drift (26).

Since F1 male individuals were backcrossed only to *B. mori* females (**Fig S2**), analysis of the BC1 panel can only detect loci for which the *B. mandarina* allele has a substantial effect in heterozygotes. To alleviate this limitation, we performed QTL analysis of the F2 mapping population. This F2 QTL scan found only one locus with significant effects on caudal horn length, Chr4 (**Table S2**, **Fig S3**), which overlaps the largest QTL observed in the BC1 analysis and shows consistent effect size with the BC1 Chr4 QTL. The effect size of the F2 Chr4 QTL is consistent with the findings from the BC1 cross. Furthermore, we independently verified the Chr4 QTL by phenotyping consomic (and semi-consomic) introgression strains of Chr4 (see **Fig S4**). Conspicuously absent from the F2 QTL scan are the additional QTL detected in the BC1 mapping panel. The smaller mapping panel for the F2 analysis may explain the relatively coarse spatial resolution of the Chr4 QTL and the absence of the seven other QTL detected in the BC1 analysis. However, the proportion of *B. mandarina* ancestry on BC1 QTL-bearing chromosomes — excluding Chr4— is a significant predictor of caudal horn length (**Table S2**, p-value = 3.4e-7), suggesting that loci on these chromosomes contribute to the trait difference despite not reaching significance in the F2 QTL analysis.

Evidence for additional loci beyond mapped QTL. The above analyses provide strong evidence for at least eight loci contributing to the caudal horn length difference between species. However, how many more loci might contribute remains unclear. Notably, the proportion of *B. mandarina* ancestry on the remaining non-QTL-bearing chromosomes is also significant predictor of caudal horn length in the F2 mapping panel (**Table S2**, p-value = 4.3e-10), consistent with a model in which many small effect loci also contribute to the morphological difference between species. To investigate this further, we carried out a regression analysis of caudal horn length as a function

of per chromosome *B. mandarina* ancestry (**Fig S5**). This analysis reveals that the proportions of *B. mandarina* ancestry on Chr3 and Chr6 are significant predictors of increased caudal horn length in the BC1 mapping panel, in addition to the QTL already identified by QTL mapping (**Fig S5B**). Even after accounting for QTL-bearing chromosomes and effects of ancestry on chromosomes 3 and 6, a significant positive correlation between caudal horn length and *B. mandarina* ancestry persists in the F2 mapping population. This indicates the presence of many diffusely-distributed small-effect caudal horn-shortening alleles that have disproportionately accumulated in the *B. mori* lineage. Thus, while the horn trait difference is clearly dominated by an oligogenic architecture, additional loci on non-QTL bearing chromosomes also make a small but significant contribution to variation in this trait.

Two Wnt-family genes exhibit caudal horn-specific cis-regulatory evolution. The 1.5 LOD (Logarithm of the Odds) interval for the BC1 Chr4 QTL region contains 17 annotated genes (**Table S3**). Among these is a cluster of four *Wnt*-family genes (**Fig 2D**), a family of secreted growth factor proteins with diverse roles in morphological development in animals (27, 28). *Wnt* genes are highly conserved across animals, and this cluster (*Wnt9*, *Wnt1*, *Wnt6* and *Wnt10*) is syntenic with orthologous genes in the *Drosophila melanogaster* genome (**Table S3**). The QTL region is syntenic in the two *Bombyx* species, with no evidence of an inversion or large insertions/deletions.

Given the presence of the *Wnt* gene cluster in the Chr4 QTL region, we speculated that differences in tissue-specific regulation of one or more of these *Wnt* genes may account for species differences in caudal horn size. To test this hypothesis, we investigated patterns of tissue-specific expression for 17 genes in the Chr4 QTL 1.5 LOD interval. First, we carried out RNA-seq to identify segment-specific differential expression between the two species (**Table S4**). We examined early-stage caterpillars (second instar, L2) because the difference in caudal horn length between the species is already visible when they hatch (**Fig S1B**), becoming more pronounced in later larval stages (**Fig S1C and S1D**). We detected 1306 transcripts with segment-specific expression divergence between species (**Supplemental Data 2**). Out of these, 121 transcripts overlap the identified QTL regions. Interestingly, this analysis reveals that only *Wnt6* exhibits significant species- and tissue-specific differential expression, with a two-fold upregulation in the eighth abdominal (A8) segment of *B. mandarina* relative to *B. mori* in the Chr4 QTL (**Fig S6A, Table S4**).

However, bulk-tissue RNA-seq-based differential expression analysis has limited statistical power for genes with low expression levels like this Chr4 cluster of *Wnt*-family genes (**Fig S6A**). Moreover, between-species comparisons of gene expression can be difficult to interpret due to species-specific differences in the trans-regulatory environment and other differences in development (e.g. cell number, the timing of development, etc.). To identify genes with cis-regulatory divergence between species, we examined allele-specific expression (ASE) in F1 hybrids, which compares the expression of two alleles in a common trans-environment (29).

To assay ASE, we used a targeted PCR-based approach (see Methods) and further dissected the A8 segment into the caudal horn structure itself (CH) versus the remaining "non-horn" A8 tissue (**Fig 3A**). This analysis reveals that only two genes, *Wnt1* and *Wnt6*, exhibit tissue-specific allele-specific expression in the fifth instar (L5) of F1 hybrid caterpillars (**Fig 3B**, **Table S5**). Specifically, both genes exhibit a caudal horn-specific down-regulation of the *B. mori* allele relative to the *B. mandarina* allele. A similar trend is observed in the F1 hybrid caterpillars at the first instar (L1) stage when the between-species caudal horn length difference is less pronounced (**Fig S6B; Table S5**). These results show that the cis-regulatory elements of *Wnt1* and *Wnt6* have diverged between these species, suggesting that differences in their tissue-specific expression may contribute to the species difference in caudal horn length. Notably, the Wnt1 and Wnt6 proteins of *B. mori* and *B. mandarina* are identical in amino acid sequence, indicating that any functional differences between the species involving these genes are solely due to cis-regulatory differences in gene expression.

To examine temporal patterns of *Wnt1* and *Wnt6* expression, we used reverse transcription quantitative PCR (RT-qPCR) to measure relative transcript abundance in integumentary tissue from A8 and A7 segments of *B. mori* and *B. mandarina*. This analysis (**Fig 3C**; **Fig S6C**) revealed several interspecific differences in expression dynamics. First, both *Wnt1* and *Wnt6* are generally expressed at higher levels in the caudal horn bearing A8 segment. Second, expression of both genes is consistently higher in *B. mandarina* than in *B. mori*, especially in the A8 segment. Third, this species difference emerges earlier for *Wnt6* and peaks for both genes at the onset of the molt preceding the L5. These findings suggest that allele-specific expression differences measured during the fifth instar (**Fig 3B**) may underestimate the divergence present at the end of the fourth instar. Specifically, *Wnt1* expression was highest in the caudal segments of *B. mandarina* on day 3 of the fourth instar, and at this time point *Wnt1* levels were also elevated in the caudal segments of both species relative to non-caudal segments. Together, the results support the idea that reduced *Wnt1* and/or *Wnt6* expression in the caudal segment of *B. mori* may contribute to its shorter horn phenotype.

Functional analyses reveal that Wnt1 and Wnt6 contribute to caudal horn length evolution. While we have established that both *Wnt1* and *Wnt6* are down-regulated in the caudal horn of *B. mori* relative to *B. mandarina*, expression studies alone cannot determine whether one or both genes have a causal effect on horn growth. Thus, to functionally validate the role of *Wnt1* and *Wnt6* in the evolved caudal horn difference between species, we used allele-specific CRISPR/Cas9-mediated gene knockouts of *B. mandarina* alleles (23) . We crossed injected (G0) females of semi-consomic line T04 ($chr4^{mand}/chr4^{mori}$) to *B. mori* p50T males to generate G1 larvae. G1 females whose *B. mandarina*-derived *Wnt1* or *Wnt6* is disrupted by small frameshift causing premature stop codon were crossed to p50T males to establish *B. mandarina*-allele-specific knockout mutants (**Fig S7**). Knocking out the *B. mandarina*-derived allele of *Wnt1* in hybrids results in a 51% reduction in caudal horn length (Tukey's HSD, $p<0.001$; **Fig 4A**). Knocking out the *B. mandarina*-derived allele of *Wnt6* also results in a reduction in horn length, but the effect (a 7% reduction) is substantially smaller (Tukey's HSD, $p<0.05$; **Fig 4A**). If *B. mori* represents the derived state, our results suggest that the down-regulation of *Wnt1* in *B. mori* contributes substantially to its reduced caudal horn length relative to *B. mandarina* (**Fig 4B**).

Discussion

The role of Wnt1 and Wnt6 in morphological divergence between species. We investigated the molecular mechanisms underlying the diversification of a conspicuous larval structure —the caudal horn— in Bombycoidea caterpillars. Our findings highlight how morphological divergence between species can result from tissue-specific regulatory changes affecting major upstream developmental genes. Specifically, we show that cis-regulatory downregulation of two *Wnt*-family genes, *Wnt1* and *Wnt6*, in the developing caudal horn of *B. mori* is the single largest contributing factor to the reduction in caudal horn length in this species. These genes, and the signaling pathways they regulate, are well known for their roles in limb and appendage development (27, 30, 31) . Moreover, cis-regulatory evolution of *Wnt1* and *WntA* has previously been linked to morphological (pigmentation) differences among insect species (32–34) .

The regulation of expression and functional roles of *Wnt*-family genes are complex (34–36). In insects, *Wnt1* and *Wnt6* share high sequence similarity, are physically adjacent in the genome, and exhibit overlapping expression domains. These features have led to the hypothesis that the two genes are at least partially co-regulated and may act redundantly in some developmental contexts (37–39). Indeed, at least one shared enhancer for *Wnt1* and *Wnt6* has previously been identified in *D. melanogaster* (40).

We find that both *Wnt1* and *Wnt6* are down-regulated in the *B. mori* caudal horn, relative to *B. mandarina*, suggesting that the underlying cis-regulatory changes may affect a shared horn-specific enhancer. Allele-specific knockouts further reveal that both *Wnt1* and *Wnt6* contribute to

horn development—though to differing degrees—supporting the idea of partial redundancy (**Fig 4**). The larger effect of *Wnt1* on caudal horn size in allele-specific knockout experiments suggests that it more functionally potent or dosage-sensitive in this context. These findings contribute to a small but growing list of examples in which cis-regulatory changes in major upstream developmental genes can underlie phenotypic divergence between closely related and domesticated species (**Table S6**).

Our results also underscore how regulatory modularity enables the resolution of developmental trade-offs associated with morphological trait divergence. The tissue-specific downregulation observed in *B. mori* illustrates how spatially restricted regulatory changes can decouple traits, allowing selection to act on horn size without potentially negative pleiotropic effects. Such modularity is a key feature of evolvability and exemplifies the utility of tissue-specific enhancers in facilitating adaptive change.

Large effect loci contribute to the evolution of the caudal horn in Bombyx. Although domestication differs from natural selection, it nonetheless offers a powerful framework for studying rapid evolutionary change under strong and often directional selective pressures (41). While some domestication traits are Mendelian, others involve more complex, quantitative architectures. Our QTL mapping analysis suggests that, in addition to *Wnt1*/*Wnt6*, at least seven more loci with smaller effects contribute to horn length variation. The three largest QTL jointly account for 27% of the difference in mean caudal horn between species, indicating that multiple loci of moderate-to-large effect explain a substantial portion of the phenotype. The oligogenic architecture of this domestication-associated trait difference resembles that of at least some traits shaped by natural selection, such as pelvic spine reduction in stickleback (42) and sexually dimorphic pigmentation in *Drosophila* (43). Additionally, we find that QTL loci act in concert with a small but measurable polygenic component. While few studies have quantified the relative contribution of the genomic background in detail, it is increasingly likely that a polygenic contribution to trait differences is a common, if often overlooked, feature of morphological divergence between species (see, for example, (44)).

Evolutionary forces shaping caudal horn evolution. The selective pressures driving caudal horn reduction in *B. mori* remain uncertain. Direct selection on horn length during domestication is unlikely. However, the consistent direction of effect across all eight QTL—where *B. mandarina* alleles increase horn length—argues against a purely neutral model (26, 45). One possibility is that horn reduction occurred as a correlated response to selection on other traits. Alternatively, the horn may have become maladaptive in the domesticated environment. The repeated gain and loss of horn-like structures across wild Bombycoidea species suggests that natural selection has repeatedly acted on this trait, potentially targeting similar developmental pathways.

Changes in *Wnt*-family gene expression have previously been implicated in morphological differences among closely-related species (32–34, 46). In Lepidoptera, *Wnt1* expression has been linked to variation in pigmentation (47) and to the formation of protruding structures (48). For example, the ectopic expression of *Wnt1* can induce protruding outgrowths in the *B. mori Knobbed* mutant larvae (48). Our results extend these findings by showing that tissue-specific downregulation of *Wnt1* in the developing caudal horn, also a protruding structure in caterpillars, is linked to cis-regulatory evolution of *Wnt1* itself, rather than changes to trans-acting factors. A key next step will be to identify the precise cis-regulatory elements responsible for *Wnt1*/*Wnt6* downregulation in *B. mori*. It is plausible that similar regulatory modules have been repeatedly co-opted for morphological innovation across Lepidoptera (**Fig 1**). Comparative studies in other species could reveal whether parallel morphological evolution has been driven by convergent changes in *Wnt* gene regulation.

Conclusion. This study integrates quantitative genetics with functional analyses to reveal the molecular basis of a conspicuous morphological trait difference distinguishing closely related species. We demonstrate that spatially precise regulatory changes in key developmental genes—*Wnt1* and *Wnt6*—underlie horn reduction in *B. mori*. These results highlight how cis-regulatory evolution can drive morphological divergence while minimizing pleiotropic effects, emphasizing the role of enhancer modularity in enabling adaptive evolution. This principle is likely to be broadly applicable across systems and taxa in evolutionary developmental biology.

Materials and Methods

Phylogenetic relationships

A cladogram for representative Lepidopteran species was constructed based on phylogenetic reconstructions of the Noctuoidea (49) the Bombicoidea (50) and the Papilonidea (51) and a broader phylogeny including all three groups (52). A cladogram for the Bombicidae was reconstructed based on several recent phylogenetic reconstructions of members of this group (53–55).

Sample collection

Bombyx mori strains c51, f35, g53, o56, p20, p21, p22, T04, and CT04 were provided from Kyushu University supported by the National BioResource (https://shigen.nig.ac.jp/silkwormbase/). *B. mori* strain p50T and *B. mandarina* strain Sakado were maintained at the University of Tokyo. For the BC1 mapping panel, F1 males were generated by crossing *B. mori* (p50T) females to *B. mandarina* (Sakado) males (**Fig S2**). We crossed F1 males to females *B. mori* p50T, generating BC_1 progeny. For the F2 mapping panel, *B. mori* p50T males were crossed with to *B. mandarina* Sakado females to produce an F1 generation, and then F1 males and females were crossed to produce an F2 generation (**Fig S2**). We phenotyped and genotyped 696 BC1 and 327 F2 caterpillars as outlined below.

Rearing and phenotyping

Larvae were reared on white mulberry (*Morus alba*) leaves or an artificial diet SilkMate PS (Nosan, Japan) at 25 ºC with a 12-hour light: 12-hour dark light cycle. We weighed and photographed fifth instar larvae at day 0 for subsequent phenotyping. Caudal horn lengths were measured from photographs by marking two points at the base of the horn and a third point at the tip of the horn using either a custom MATLAB script or ImageJ (56). For each horn, we defined a triangle extending upward from the base of the horn using three points (1, 2, 3), and an additional segment defined by a 4th point at the tip of the horn (**Fig S1C**). Length (L) was then calculated as,

$$L = \frac{|(X_2 - X_1)(Y_1 - Y_3) - (X_1 - X_3)(Y_2 - Y_1)|}{\sqrt{(X_2 - X_1)^2 + (Y_2 - Y_1)^2}} + \sqrt{(X_4 - X_3)^2 + (Y_4 - Y_3)^2},$$

where X_k and Y_k are coordinates of point k. The phenotype distributions of the BC1 and F2 are near normal distributions (Shapiro-Wilk test $p = 0.14$ and $p = 0.10$, respectively).

Divergence dating

Nei's π within species and *dxy* between species using 3 *B. mori* strains (b20, DRR059699; N4, DRR059712; p50T, GCF_014905235.1) and 3 *B. mandarina* strains (Japan origin Sakado, DRR059710; Japan origin Oki, DRR059709; China origin, GCF_003987935.1) respectively. All samples had > 30x coverage. Strains were adapter-trimmed and aligned to the p50T genome assembly using bwa mem. Duplicate and secondary alignment reads were removed from downstream analysis. Variants were called across the samples using bcftools mpileup. SNPs overlapping repetitive regions identified by RepeatMasker and with GQ<30, MQ<30, within 3bp of an indel, and with missing fraction > 0.5 were removed. Remaining SNPs across all autosomes, accounting for masked regions, were used to calculate diversity through scripts from https://github.com/YourePrettyGood/RandomScripts. Approximate time to coalescence was estimated as T=(dxy- π_Bmand)/2μ where the mutation rate μ is 2.2x10^-9.

Genome-wide ancestry assignment

We used Multiplexed Shotgun Genotyping (57) to carry out genome-wide ancestry assignment of recombinant progeny. Genomic DNA was extracted from the legs of the adults using the Quick-DNA extraction kit (Zymo Research, USA). Whole genome short-read Illumina-style libraries were generated using a Tn5-based "tagmentation" method (58) . For each individual, 4–15 ng of genomic DNA (measured using Synergy MX Microplate Reader [BioTek, USA]) was digested with Tn5 that was pre-charged with Illumina-style adapters. Individuals were indexed by PCR amplification (18 cycles) using combinations of Illumina-compatible i5 and i7 indexed PCR primers. Library sequencing for BC1 was performed on HiSeq 2500 (Illumina, USA) at the Princeton University Genomics Core Facility, yielding 75 nucleotide single-end reads. Libraries for the F2 were sequenced on a HiSeq 4000 (Illumina, USA) at the Weill-Cornell Medical College Genomics Resources Core Facility, yielding 150 nucleotide paired-end reads, and read 1 was used for downstream analysis. Reads were de-multiplexed and adapters removed using Trim Galore (bioinformatics.babraham.ac.uk/projects/trim_galore/). The average number of reads per individual was 572,000 and individuals with fewer than 100,000 reads were discarded.

A *B. mori* p50T strain genome assembly (BHWX01000001-BHWX01000696, 2016) from Silkbase (59), and a *B. mandarina* Sakado strain genome assembly (GCA_030267445.2, NCBI) were used as parental reference genomes. Repetitive regions were identified and masked in the *B. mori* and *B. mandarina* genomes using RepeatMasker v4.1.2 with the species set to "bombyx". We also masked sites that were polymorphic in either p50T or Sakado strains. To identify polymorphic sites within each strain, paired-end short-read Illumina reads of a p50T male (DRR064025; NCBI) and two Sakado samples (DRR059710, DRR093001; NCBI) were adapter-trimmed using Trim Galore v0.6.10 and aligned to the *B. mori* genome (bwa v0.7.17) (60) and variants were called using bcftools mpileup v1.16 (61) . Sites were removed based on the following quality filters: MQ <30, GQ<25, removing any SNPs within 5 bp of an indel (--SnpGap 5:indel), and where the read-depth was less than half (<0.5x) or more than two times (>2x) the average total read depth.

MSG was run with *B. mori* designated as parent1 and *B. mandarina* as parent2, using the following parameters: deltapar1 = 0.01, deltapar2 = 0.05, recRate = 28, rfac = 0.0001, and priors set to (0.25, 0.5, 0.25) for F2 crosses and (0, 0.5, 0.5) for BC1 crosses. For each individual, genotypes were assigned as missing (i.e., "NA") if the posterior probability was below 90%. Additionally, we masked genomic regions between ancestry switches within an individual that occurred less than 1 Mbp apart. Finally, sites with more than 20% missing genotypes across individuals within each cross. This filtering yielded a set of 1,595,348 markers shared between the BC1 and F2 datasets. To reduce redundancy, we applied marker thinning using pull_thin (https://github.com/andrewtaverner/pull_thin) with the following settings: numMarkers = 5000, ignoreNan = True, exclude_ambiguous_AIMs = True, and autosome_prior = NA. A final set of 140,000 markers was retained for QTL analysis.

Quantitative Trait Locus (QTL) analysis

We performed two separate QTL analyses using R/qtl (62) with genotype and caudal horn lengths for 327 F2 and 694 BC1 individuals. The Haley-Knott regression method (63) was used for QTL mapping with sex, weight (a proxy for size), and genome-wide *B. mandarina* ancestry as covariates. Ancestry was calculated as the proportion of the genome assigned as *B. mandarina*-derived accounting for diploidy. Ancestry was calculated excluding chromosomes that carried a significant QTL. Genome-wide 5% significance thresholds were determined by 1000 phenotype permutations (64). These were estimated as LOD > 3.03 and LOD > 3.63 for the BC1 and F2 analyses, respectively. For each significant QTL, a 1.5 LOD support interval spanning the maxLOD peak was considered the candidate region (65). Variance explained was calculated using the function fitqtl (62).

Differential Expression analysis

Caudal and non-caudal segments (A8 and A7, respectively; **Fig 3B**) were dissected from caterpillars before the onset of the second (L2) instar. Three replicate pools of eight individuals were generated for each species and segment (except the *B. mori* non-caudal segments, for which there are two replicates). Samples were stored at –80ºC in RNAlater (Thermo Fisher Scientific). RNA was extracted using the RNAeasy kit (QIAGEN) and RNA-seq libraries were prepared using TruSeq RNA Library Preparation Kit v2 (Illumina). Libraries were sequenced on HiSeq 4000 (Illumina) at the Weill-Cornell Medical College Genomics Resources Core Facility, yielding 312 million 150 nucleotide single-end reads. This corresponds to an average of 28 million reads per replicate and tissue. Reads were mapped to the *B. mori* annotated transcriptome (59) using STAR (66) . Read count output from STAR was then imported into DESeq2 (67) for differential expression analysis.

Differential expression analysis was performed to detect transcripts with caudal (A8) and non-caudal (A7) segment-specific expression differences between the species. To this end, the model used to analyze all tissue samples from all replicates was: ~Species:Replicate + Species*Tissue, where "Species" is *B. mori* or *B. mandarina* and "Tissue" is caudal (A8) or noncaudal (A7). The first term of the model defines Replicate as a nested variable within Species and accounts for the fact that caudal and non-caudal segments were sampled from the same individuals. Our quantity of interest is the second term, which accounts for potential interactions between Species and Tissue (i.e. species- and tissue-specific differential expression).

Allele-specific expression (ASE) analysis

To investigate allele-specific expression patterns for the genes within the Chr4 QTL, we extracted RNA from relevant tissues in *B. mori* p50T × *B. mandarina* Sakado F1 hybrids. The caudal segment (A8) was dissected from first (L1) and fifth (L5) larval instars and further dissected into caudal horn (CH) and "non-horn" A8 tissue (**Fig 3B**). Four replicate pools of 10 individuals were sampled for each segment and instar. Samples were stored in RNAlater™ Stabilization Solution (Thermo Fisher Scientific), and total RNA was extracted using TRIzol (Thermo Fisher Scientific), RNeasy columns (QIAGEN) and DNaseI (Thermo Fisher Scientific). Total RNA from each sample was used to create cDNA using SuperScript IV VILO® (Thermo Fisher Scientific). The conversion to cDNA was repeated three times for each sample representing technical replicates.

We quantified relative allele abundance using a targeted multiplexed PCR-sequencing approach. For each of 13 genes in the Chr4 QTL interval we tested (see **Table S3**), PCR primers were designed to target a genic region that spans at least one SNP distinguishing the two species (**Table S7**). We PCR-amplified these amplicons from F1 cDNA samples using the following reaction conditions: 94°C (30″), 95°C (15″), 60°C (30″), 68°C (45″), 68°C (5′) for 15 cycles. To allow multiplexed Illumina sequencing, we incorporated a second set of universal i5 and i7 Illumina-style indexes using the following conditions: 72 °C (3′), 94°C (10″) 62°C (15″) 68°C (30″) 68°C (5′) for 12 cycles. After removing primer dimers with DNA clean & concentrator (D4030), indexed amplicons were pooled and sequenced on a MiSeq (Illumina) using Reagent Micro Kit v2 (Illumina), 300 Cycles (MS-103-1002). Reads were demultiplexed and, for each replicate, we counted the number of reads corresponding to each species-specific SNP. Genomic DNA (gDNA) samples for F1 hybrid individuals were also assayed using the same primer pairs to account for potential preferential amplification of one allele. The inverted beta-binomial (ibb) test for paired-count data (68) was used to identify significant abundance differences between *B. mandarina* and *B. mori* alleles for each gene. We used this test to both establish whether the *B. mandarina*/*B. mori* allele ratio for cDNA is significantly different than 1 (using gDNA-derived counts as a reference) and whether the *B. mandarina*/*B. mori* allele ratio for cDNA is significantly different in the caudal horn versus non-horn tissue.

Reverse Transcription quantitative PCR (RT-qPCR)

To quantify the relative abundance of *Wnt1* and *Wnt6* RNA in a time course of larval development, we used a RT-qPCR approach. Total RNA was isolated from integuments of caudal

(A8) and non-caudal (A7) segments of *B. mori* and *B. mandarina* using TRIzol (Thermo Fisher Scientific). Reverse transcription was performed using the oligo (dT) primer and avian myeloblastosis virus Reverse Transcriptase contained in the RNA PCR kit (TaKaRa, Japan). We conducted RT-qPCR using the Kapa SYBR FAST qPCR kit (Kapa Biosystems, USA) and StepOnePlus Real-time PCR System (Applied Biosystems, USA). RNA abundance is quantified relative to *ribosomal protein 49* (*rp49*). Primer sets are listed in **Table S8**.

CRISPR/Cas9-mediated allele-specific knockouts.

To evaluate the effects of *Wnt1* and *Wnt6* expression on caudal horn development, we used CRISPR/Cas9-mediated allele-specific knockout approach (23). Instead of F1 hybrids, we instead used the T04 semi-consomic strain, which is heterozygous *B. mori* (p50T) / *B. mandarina* (Sakado) for Chr4 in an otherwise *B. mori* (p50T) genomic background ((69) ; see **Fig S4**).

We identified Cas9 PAM-sites that differed in sequence between *B. mori* and *B. mandarina* and designed CRISPR-RNA (crRNA) targeting *B. mandarina*-specific sequences (**Fig S6**) (23). To obtain non-diapausing eggs, we first incubated T04 eggs at 15ºC under continuous darkness until they hatch (70). The hatched larvae were then reared under continuous 16h-light/8h-dark at 25 °C and crossed adult females to p50T males and collected fertilized eggs. A mixture of crRNA (200 ng/μL; FASMAC, Japan), trans-activating crRNA (tracrRNA) (200 ng/μL; FASMAC), and Cas9 Nuclease protein NLS (600 ng/μL; NIPPON GENE) was injected into eggs within 3 hours of oviposition (71) . Injected embryos were then incubated at 25 °C in a humidified Petri dish until hatching. Adult generation 0 (G0) females were crossed with the wild-type p50T males to obtain generation 1 (G1) progeny. Genomic DNA was extracted from the G1 individuals by the HotSHOT method (72), and PCR was performed using KOD One (TOYOBO, Japan) or MightyAmp DNA Polymerase Ver.3 (TaKaRa). Mutations at the targeted site were detected by heteroduplex mobility assay using the MultiNA microchip electrophoresis system (SHIMADZU, Japan) with the DNA-500 reagent kit (73, 74). The PCR products were also cloned into pGEM-T Easy Vector (Promega, USA) and Sanger-sequenced using the FASMAC sequencing service. G1 females carrying a 7-nucleotide deletion in *B. mandarina*-derived *Wnt1* and 2-nucleotide deletion in *B. mandarina*-derived *Wnt6* were crossed to wild-type p50T males, respectively, to establish *B. mandarina*-allele-specific knockout mutants (**Fig S7**). Both mutations result in frameshifts and premature stop codons. Mutant larvae were weighed and the caudal horn length measured as described above and then genotyped using PCR. RNA oligos and PCR primer sets were listed in **Table S9**.

Effects of chromosome-level ancestry on caudal horn length

We analyzed ancestry and its relationship to caudal horn length using the standardized coefficients from the linear regression model as measures of effect size (R v.4.0.2). We adjusted p-values using a Bonferroni correction for the number of chromosomes. Akaike information criterion (AIC) model selection was used to evaluate the association between ancestry and caudal horn length (**Fig S5**) with ancestry on all chromosomes included as independent variables.

Acknowledgments:

Maria Gutin laid the preliminary groundwork for the project as part of her Ph. D. dissertation **(75)**. We thank Toru Shimada and Shuji Shigenobu for helpful comments during the early stages of this project. We also thank the Institute for Sustainable Agro ecosystem Services, the University of Tokyo, for facilitating the mulberry cultivation and the Biotron Facility at the University of Tokyo for rearing the silkworms. We thank Lina Ruiz and Njeri Sparman for help with insect husbandry.

Funding:

This work was partly supported by National Institutes of Health grants R01 GM114093, R01 GM112758 and R01 GM115523 to PA. This work was also supported by JSPS KAKENHI grant numbers JP20J22954 to KT and JP20H02997 to TK.

Author contributions:
Designed research (KT,AP,TK,PA); Performed research (KT, AP, YK, MLA, JCH, LK, LP, PRR, AMT); Analyzed data (KT ,AP ,YK ,AMT, PA); Wrote the paper (KT, AP, TK, PA).

Competing interests: The authors declare no competing interests.

Data and materials availability:
Code and analysis scripts are available at https://github.com/apinharanda/Bombyx_caudalHorn.
Sequencing data will be deposited in the NCBI Sequence Read Archive under BioProject accession [PRJNAxxxxxx], with associated BioSample accession(s) [SAMNxxxxxx], and will be made publicly available upon completion of the submission process (currently under submission ID: SUB15460842).

Supplementary Materials:
Figs. S1 to S8
Tables S1 to S9
Data S1 to S3

References:
1. N. Shubin, C. Tabin, S. Carroll, Fossils, genes and the evolution of animal limbs. *Nature* **388**, 639–648 (1997).
2. S. B. Carroll, J. K. Grenier, S. D. Weatherbee, *From DNA to diversity : molecular genetics and the evolution of animal design*, Blackwell, Ed., 2nd Ed. (Blackwell, 2004).
3. E. H. Davidson, I. S. Peter, *Genomic Control Process: Development and Evolution* (Academic Press, 2015).
4. V. Courtier-Orgogozo, L. Arnoult, S. R. Prigent, S. Wiltgen, A. Martin, Gephebase, a database of genotype–phenotype relationships for natural and domesticated variation in Eukaryotes. *Nucleic Acids Res.* **48**, D696–D703 (2020).
5. H. A. Orr, J. A. Coyne, The genetics of adaptation: a reassessment. *Am. Nat.* **140**, 725–42 (1992).
6. D. Stern, *Evolution, development, and the predictable genome* (Roberts and Company Publishers, 2010).
7. A. Martin, V. Orgogozo, THE LOCI OF REPEATED EVOLUTION: A CATALOG OF GENETIC HOTSPOTS OF PHENOTYPIC VARIATION. *Evolution* **67**, 1235–1250 (2013).
8. D. J. Emlen, J. Marangelo, B. Ball, C. W. Cunningham, DIVERSITY IN THE WEAPONS OF SEXUAL SELECTION: HORN EVOLUTION IN THE BEETLE GENUS ONTHOPHAGUS (COLEOPTERA: SCARABAEIDAE). *Evolution* **59**, 1060–1084 (2005).
9. P. David, T. Bjorksten, K. Fowler, A. Pomiankowski, Condition-dependent signalling of genetic variation in stalk-eyed flies. *Nature* **406**, 186–188 (2000).
10. K. HASHIMOTO, F. HAYASHI, Structure and function of the large pronotal horn of the sand-living anthicid beetle Mecynotarsus tenuipes. *Entomol. Sci.* **15**, 274–279 (2012).
11. I. Kandori, K. Tsuchihara, T. A. Suzuki, T. Yokoi, D. R. Papaj, Long Frontal Projections Help Battus philenor (Lepidoptera: Papilionidae) Larvae Find Host Plants. *PLoS ONE* **10**, e0131596 (2015).
12. I. Kandori, *et al.*, Long horns protect Hestina japonica butterfly larvae from their natural enemies. *Sci. Rep.* **12**, 2835 (2022).
13. Packard, Cockerell, *Monograph of the Bombycine Moths of North America: Family Ceratocampidæ, subfamily Ceratocampinæ*, U. S. G. P. Office, Ed. (1905).
14. Z. Liu, X. Cao, Z. Liu, X. Cao, Rondotia melanoleuca sp. nov., a new wild-mulberry silkworm from China (Lepidoptera, Bombycidae). *Nota Lepidopterol.* **47**, 49–56 (2024).

15. T. J. Hossie, T. N. Sherratt, D. H. Janzen, W. Hallwachs, An eyespot that "blinks": an open and shut case of eye mimicry in Eumorpha caterpillars (Lepidoptera: Sphingidae). *J. Nat. Hist.* **47**, 2915–2926 (2013).
16. W. Sun, *et al.*, Phylogeny and evolutionary history of the silkworm. *Sci. China Life Sci.* **55**, 483–496 (2012).
17. S.-Y. Yang, *et al.*, Demographic history and gene flow during silkworm domestication. *BMC Evol. Biol.* **14**, 185 (2014).
18. M. Han, *et al.*, Mutation Rate and Spectrum of the Silkworm in Normal and Temperature Stress Conditions. *Genes* **14**, 649 (2023).
19. H. Xiang, *et al.*, The evolutionary road from wild moth to domestic silkworm. *Nat. Ecol. Evol.* **2**, 1268–1279 (2018).
20. N. Kômoto, Behavior of the larvae of wild mulberry silkworm Bombyx mandarina, domesticated silkworm B. mori and their hybrid. *J. Insect Biotechnol. Sericology* **86**, 1_017-1_020 (2017).
21. K. Lu, *et al.*, Flight Muscle and Wing Mechanical Properties are Involved in Flightlessness of the Domestic Silkmoth, Bombyx mori. *Insects* **11**, 220 (2020).
22. S.-M. Fang, Q.-Z. Zhou, Q.-Y. Yu, Z. Zhang, Genetic and genomic analysis for cocoon yield traits in silkworm. *Sci. Rep.* **10**, 5682 (2020).
23. K. Tomihara, P. Andolfatto, T. Kiuchi, Allele-specific knockouts reveal a role for apontic-like in the evolutionary loss of larval melanin pigmentation in the domesticated silkworm, Bombyx mori. *Insect Mol. Biol.* **31**, 701–710 (2022).
24. S. Bisch-Knaden, T. Daimon, T. Shimada, B. S. Hansson, S. Sachse, Anatomical and functional analysis of domestication effects on the olfactory system of the silkmoth Bombyx mori. *Proc. R. Soc. B: Biol. Sci.* **281**, 20132582 (2014).
25. H.-S. Yu, *et al.*, Evidence of Selection at Melanin Synthesis Pathway Loci during Silkworm Domestication. *Mol. Biol. Evol.* **28**, 1785–1799 (2011).
26. H. A. Orr, Testing Natural Selection vs. Genetic Drift in Phenotypic Evolution Using Quantitative Trait Locus Data. *Genetics* **149**, 2099–2104 (1998).
27. S. Murat, C. Hopfen, A. P. McGregor, The function and evolution of Wnt genes in arthropods. *Arthropod Struct. Dev.* **39**, 446–452 (2010).
28. K. M. Loh, R. van Amerongen, R. Nusse, Generating Cellular Diversity and Spatial Form: Wnt Signaling and the Evolution of Multicellular Animals. *Dev. Cell* **38**, 643–655 (2016).
29. P. J. Wittkopp, B. K. Haerum, A. G. Clark, Evolutionary changes in cis and trans gene regulation. *Nature* **430**, 85–88 (2004).
30. C. Y. Logan, R. Nusse, THE WNT SIGNALING PATHWAY IN DEVELOPMENT AND DISEASE. *Cell Dev. Biol.* **20**, 781–810 (2004).
31. K. E. Wiese, R. Nusse, R. van Amerongen, Wnt signalling: conquering complexity. *Development* **145**, dev165902 (2018).
32. A. Martin, *et al.*, Diversification of complex butterfly wing patterns by repeated regulatory evolution of a Wnt ligand. *Proc. Natl. Acad. Sci.* **109**, 12632–12637 (2012).
33. A. Martin, R. D. Reed, Wnt signaling underlies evolution and development of the butterfly wing pattern symmetry systems. *Dev. Biol.* **395**, 367–378 (2014).
34. S. Koshikawa, *et al.*, Gain of cis-regulatory activities underlies novel domains of wingless gene expression in Drosophila. *Proc. Natl. Acad. Sci.* **112**, 7524–7529 (2015).
35. R. van Amerongen, R. Nusse, Towards an integrated view of Wnt signaling in development. *Development* **136**, 3205–3214 (2009).
36. J. E. Gleason, E. A. Szyleyko, D. M. Eisenmann, Multiple redundant Wnt signaling components function in two processes during C. elegans vulval development. *Dev. Biol.* **298**, 442–457 (2006).
37. K. Janson, E. D. Cohen, E. L. Wilder, Expression of DWnt6, DWnt10, and DFz4 during Drosophila development. *Mech. Dev.* **103**, 117–120 (2001).
38. R. Bolognesi, *et al.*, Tribolium Wnts: evidence for a larger repertoire in insects with overlapping expression patterns that suggest multiple redundant functions in embryogenesis. *Dev. Genes Evol.* **218**, 193–202 (2008).

39. R. Quinlan, M. Graf, I. Mason, A. Lumsden, C. Kiecker, Complex and dynamic patterns of Wnt pathway gene expression in the developing chick forebrain. *Neural Dev.* **4**, 35 (2009).
40. R. E. Harris, L. Setiawan, J. Saul, I. K. Hariharan, Localized epigenetic silencing of a damage-activated WNT enhancer limits regeneration in mature Drosophila imaginal discs. *eLife* **5**, e11588 (2016).
41. L. Andersson, M. Purugganan, Molecular genetic variation of animals and plants under domestication. *Proc. Natl. Acad. Sci.* **119**, e2122150119 (2022).
42. M. D. Shapiro, *et al.*, Genetic and developmental basis of evolutionary pelvic reduction in threespine sticklebacks. *Nature* **428**, 717–723 (2004).
43. Y. Liu, *et al.*, Changes throughout a Genetic Network Mask the Contribution of Hox Gene Evolution. *Curr. Biol.* **29**, 2157-2166.e6 (2019).
44. D. L. Powell, *et al.*, The Genetic Architecture of Variation in the Sexually Selected Sword Ornament and Its Evolution in Hybrid Populations. *Curr. Biol.* **31**, 923-935.e11 (2021).
45. L. K. Hayward, G. Sella, Polygenic adaptation after a sudden change in environment. *eLife* **11**, e66697 (2022).
46. D. Navon, N. Olearczyk, R. C. Albertson, Genetic and developmental basis for fin shape variation in African cichlid fishes. *Mol. Ecol.* **26**, 291–303 (2017).
47. J. Yamaguchi, *et al.*, Periodic Wnt1 expression in response to ecdysteroid generates twin-spot markings on caterpillars. *Nat. Commun.* **4**, 1857 (2013).
48. M. Edayoshi, J. Yamaguchi, H. Fujiwara, Protruding Structures on Caterpillars Are Controlled by Ectopic Wnt1 Expression. *PLoS ONE* **10**, e0121736 (2015).
49. P. Sihvonen, *et al.*, Insect taxonomy can be difficult: a noctuid moth (Agaristinae: Aletopus imperialis) and a geometrid moth (Sterrhinae: Cartaletis dargei) combined into a cryptic species complex in eastern Africa (Lepidoptera). *PeerJ* **9**, e11613 (2021).
50. I. J. Kitching, *et al.*, A global checklist of the Bombycoidea (Insecta: Lepidoptera). *Biodivers. Data J.* **6**, e22236 (2018).
51. M. Espeland, *et al.*, A Comprehensive and Dated Phylogenomic Analysis of Butterflies. *Curr. Biol.* **28**, 770-778.e5 (2018).
52. A. Y. Kawahara, *et al.*, Phylogenomics reveals the evolutionary timing and pattern of butterflies and moths. *Proc. Natl. Acad. Sci. United States Am.* **116**, 22657–22663 (2019).
53. C. A. Hamilton, *et al.*, Phylogenomics resolves major relationships and reveals significant diversification rate shifts in the evolution of silk moths and relatives. *BMC Evol. Biol.* **19**, 182 (2019).
54. M. Deng, C. Liao, Q. Chen, G. Huang, X. Wang, Phylogenetic relationships among Bombycinae (Lepidoptera, Bombycoidea, and Bombycidae) based on mitochondrial genomes. *Arch. Insect Biochem. Physiol.* **111**, e21889 (2022).
55. T. Daimon, *et al.*, Molecular phylogeny, laboratory rearing, and karyotype of the bombycid moth, Trilocha varians. *J. Insect Sci.* **12**, 49 (2012).
56. C. A. Schneider, W. S. Rasband, K. W. Eliceiri, NIH Image to ImageJ: 25 years of image analysis. *Nat. methods* **9**, 671–5 (2012).
57. P. Andolfatto, *et al.*, Multiplexed shotgun genotyping for rapid and efficient genetic mapping. *Genome Res.* **21**, 610–617 (2011).
58. S. Picelli, *et al.*, Tn5 transposase and tagmentation procedures for massively scaled sequencing projects. *Genome Res.* **24**, 2033–2040 (2014).
59. M. Kawamoto, *et al.*, High-quality genome assembly of the silkworm, Bombyx mori. *Insect Biochem. Mol. Biol.* **107**, 53–62 (2019).
60. H. Li, Aligning sequence reads, clone sequences and assembly contigs with BWA-MEM. *arXiv* (2013). https://doi.org/10.48550/arxiv.1303.3997.
61. P. Danecek, *et al.*, Twelve years of SAMtools and BCFtools. *GigaScience* **10**, giab008 (2021).
62. K. W. Broman, H. Wu, Ś. Sen, G. A. Churchill, R/qtl: QTL mapping in experimental crosses. *Bioinformatics* **19**, 889–890 (2003).
63. C. S. Haley, S. A. Knott, A simple regression method for mapping quantitative trait loci in line crosses using flanking markers. *Heredity* **69**, 315–324 (1992).

700 64. G. A. Churchill, R. W. Doerge, Empirical threshold values for quantitative trait mapping. *Genetics* **138**, 963–971 (1994).
65. J. Dupuis, D. Siegmund, Statistical Methods for Mapping Quantitative Trait Loci From a Dense Set of Markers. *Genetics* **151**, 373–386 (1999).
66. A. Dobin, *et al.*, STAR: ultrafast universal RNA-seq aligner. *Bioinformatics* **29**, 15–21 (2012).
705 67. M. I. Love, W. Huber, S. Anders, Moderated estimation of fold change and dispersion for RNA-seq data with DESeq2. *Genome Biol.* **15**, 550 (2014).
68. T. V. Pham, C. R. Jimenez, An accurate paired sample test for count data. *Bioinformatics* **28**, i596–i602 (2012).
69. T. Fujii, *et al.*, Development of interspecific semiconsomic strains between the domesticated
710 silkworm, Bombyx mori and the wild silkworm, B. mandarina. *J. Insect Biotechnol. Sericology* **90**, 2_033-2_040 (2021).
70. M. Kogure, The Influence Of Light And Temperature On Certain Characters Of The Silkworm, Bombyx Mori. *J. Fac. Agric., Kyushu Univ.* **4**, 1–93 (1933).
71. J. Yamaguchi, T. Mizoguchi, H. Fujiwara, siRNAs Induce Efficient RNAi Response in Bombyx
715 mori Embryos. *PLoS ONE* **6**, e25469 (2011).
72. G. E. Truett, *et al.*, Preparation of PCR-Quality Mouse Genomic DNA with Hot Sodium Hydroxide and Tris (HotSHOT). *BioTechniques* **29**, 52–54 (2000).
73. S. Ota, *et al.*, Efficient identification of TALEN-mediated genome modifications using heteroduplex mobility assays. *Genes Cells* **18**, 450–458 (2013).
720 74. S. Ansai, *et al.*, Design, evaluation, and screening methods for efficient targeted mutagenesis with transcription activator-like effector nucleases in medaka. *Dev., Growth Differ.* **56**, 98–107 (2014).
75. Gutin, "THE GENETICS OF MORPHOLOGICAL EVOLUTION IN SILKWORMS (BOMBYCIDAE: BOMBYX)," Princeton, NJ : Princeton University. (2019).
725

Figure legends:

Figure 1. Evolutionary diversification of Lepidopteran larval appendages.
(A) Representative morphological diversity among Lepidopteran caterpillars. Phylogenetic relationships are indicated by the cladogram and family names for each representative species are indicated (based on refs 49-51). *Bombyx* belongs to the Bombicidae (highlighted in red)
(B) Representative caudal horn diversity among species in the Bombicidae family. Shown are the posterior larval segments for each species; the cladogram depicts their phylogenetic relationships (53-55).

Figure 2. QTL analyses for caudal horn length.
(A) Distributions of caudal horn lengths (CH) in *B. mori* p50T and *B. mandarina* (Sakado) parental species and hybrids. F1 hybrids are the progeny of p50T females × Sakado males; BC1 are the progeny of p50T females and F1 males; F2 are the progeny of F1 hybrids generated by crossing *B. mori* p50T males and *B. mandarina* Sakado females.
(B) QTL LOD profile plots for caudal horn length based on the BC1 mapping panel. LOD is shown in black with a red dashed line indicating the estimated significance threshold (3.02) determined by 1000 phenotype permutations. Red arrows indicate significant QTL peaks.
(C) Caudal horn length distributions of BC1 individuals based on marker genotypes immediately under the three highest LOD peaks on chromosomes 4, 5, and 21. Caudal horn lengths are adjusted for larval weight and sex. The last panel shows caudal horn distributions of BC1 individuals whose genotypes are jointly homozygous *B. mori* or jointly heterozygous at all three QTL. The % mean length difference between mori:mori and mori:mand genotypes normalized by the mean length difference between the parental species for each peak are noted in blue.
(D) Annotation of the chromosome 4 QTL interval. Boxes indicate annotated genes within the 1.5 LOD interval (delimited by dashed lines) estimated in the BC1 QTL analysis (**Table S3**). *Wnt*-family genes are colored in orange. Coordinates are in Mega base pairs (Mbp).

Figure 3. Cis-regulatory divergence underlies species- and tissue-specific *Wnt1* and *Wnt6* expression patterns during larval development.
(A) Schematic of the sampling scheme for gene expression analyses. Total RNA was extracted from caudal horn (CH, segment A8) and non-horn tissue of the eighth abdominal segment (A8) for RNA-seq (**Fig S6A**) and targeted ASE (**Fig 3B and Fig S6B**). Total RNA from the integument of segments A7 and A8 was extracted for RNA-seq (**Fig S6A**) and the temporal expression analysis (**Fig 3C and Fig S6C**).
(B) Allele-specific expression patterns in the caudal horn of *B. mori* (p50T) × *B. mandarina* (Sakado) F1 hybrids of L5 (final) instar caterpillars. Plotted for each gene in the QTL interval (in the same order, left to right), is the log2(fold-difference) in the average *B. mori* and *B. mandarina* allele counts for the caudal horn portion of segment A8. Values larger than 0 indicate higher expression of the *B. mandarina* allele and whiskers represent two standard errors (corresponding to 95% confidence intervals among biological replicates). "CH" shows the caudal horn tissue and "A8" the non-horn tissue portion (Fig3A). A corresponding analysis of L1 (first) instar caterpillars is shown in **Fig S6B**. Significance of ASE differences between the caudal and non-caudal portions of segment A8 were evaluated using the inverted beta-binomial test (ibb) test for paired count data and significant differences are indicated with asterisks (Bonferroni corrected, **Table S5**).
(C) Temporally-elevated expression of *Wnt1* and *Wnt6* in segment A8 of *B. mandarina*. Temporal expression of *Wnt1* and *Wnt6* in the integument tissue of segment A8 during the transition between fourth and fifth instar stages of *B. mori* and *B. mandarina* caterpillar development. A corresponding analysis of segment A7 is shown in **Fig. S6C**. Relative *Wnt1* and *Wnt6* expression levels (setting *B. mori* A8 at day 0 of 4th instar = 1) were normalized to those of *ribosomal protein 49* (*rp49*). Whiskers represent two standard errors among replicates.

Figure 4. *Wnt1* and *Wnt6* CRISPR/Cas9-mediated *B. mandarina*-allele-specific knockouts significantly reduce caudal horn length.
(A) Distributions of caudal horn lengths for larvae at day 0 of the fifth instar (L5). Diagrams to the left indicate the genotypes of the strains being compared (Chr4=chromosome 4; GB=genomic background). Blue corresponds to the p50T *B. mori* background; and red to the *B. mandarina* Sakado

background. chr4$^{mand\Delta Wnt1}$/chr4^{mori} and chr4$^{mand\Delta Wnt6}$/chr4^{mori} correspond to CRISPR/Cas9-mediated *B. mandarina*-allele-specific knockouts of *Wnt1* and *Wnt6*, respectively. White points indicate individual caterpillar horn lengths, corrected for caterpillar weight (a proxy for size). Black points and whiskers correspond to means and standard errors. Letters on the right indicate groups that differ significantly in caudal horn length based on a one-way ANOVA followed by Tukey's HSD test (family-wise confidence level = 95%). A significant positive allometric relationship was observed between body weight and caudal horn length (ANCOVA: effect of weight, $p = 2.9 \times 10^{-16}$), with a significantly steeper slope in *B. mandarina* than in *B. mori* (interaction term, $p = 0.016$), see **Fig S1**.
(B) Conceptual representation of relative *Wnt1* and *Wnt6* transcriptional abundances for each genotype. Expression results (**Fig 3**) indicate that *Wnt1* and *Wnt6* have elevated transcript abundance in caudal horn tissue of stage L5 *B. mandarina* caterpillars. Knock-outs of the *B. mandarina* allele are expected to decrease (but not eliminate) expression of *Wnt1* or *Wnt6* relative to all other genotypes in the entire animal.

Figure S1. Measurement of caudal horn length variation.
(A) Caudal horn (CH) length measurements across various strains of *B. mori* and *B. mandarina* Sakado. The *B. mori* strain used in this study is p50T. Values were not adjusted for weight or sex.
(B) Neonate (day 0 of first instar) larvae of *B. mori* (left) and *B. mandarina* (right). Red arrows indicate the caudal horns. Scale bars = 1 mm.
(C) Measuring the caudal horn. Images of L5 larval caudal horns were marked at three locations (colored points) using MATLAB or ImageJ. Two purple points are laid to mark the base of the caudal horn, corresponding to $X_{1,2}$,$Y_{1,2}$ (see Methods: Rearing and Phenotyping), and the black point marks the vertex X_3,Y_3. The height of the triangle is then added to the distance between the black point and the blue point X_4,Y_4 located at the tip of the caudal horn.
(D) Caudal horn (CH) length and caterpillar weight relationship for *B. mori* (p50T) and *B. mandarina* (Sakado) at L5 stage. Values were not adjusted for weight or sex.

Figure S2. Schematic of the cross design for the BC1 and F2 mapping panels.
(A) The BC1 mapping panel. *B. mandarina* Sakado (Bmand) males were crossed to *B. mori* (Bmori) p50T females to create F1 males. F1 males were then backcrossed to *B. mori* p50T to produce BC1 progeny. Note that the W chromosome of BC1 females (red) is derived from *B. mori* p50T. The large X indicates meiotic crossing over in F1 males.
(B) The F2 mapping panel. *B. mori* p50T (Bmori) males were crossed to a *B. mandarina* (Bmand) Sakado females to create F1 males. F1 males and females were crossed to produce F2 progeny. Note that the W chromosome of F2 females (black) is derived from *B. mandarina* Sakado. The large X indicates meiotic crossing over in F1 males.

Figure S3. F2 QTL analysis and estimated QTL effect sizes.
(A) Caudal horn (CH) length distributions of BC1 individuals based for markers corresponding to maximum LOD peaks for QTLs on chromosomes 7, 9, 10, 25, and 26. Caudal horn length was adjusted for larval sex and weight. Effect sizes (in blue) are the % mean length difference between heterozygous (mori:mand) and homozugous *B. mori* (mori:mori) genotype, normalized by the mean length difference between the parental species.
(B) F2 QTL LOD profile for caudal horn length. LOD is shown in blue with the red dashed line indicating the LOD significance threshold of 3.62 determined by 1000 permutations.
(C) Superposition of BC1 (black) and F2 (blue) LOD profiles for Chr4. The vertical line and red triangle indicate the max LOD position in BC1. LOD significance threshold for BC1 is 3.02, and F2 is 3.62.
(D) Caudal horn length distributions of F2 individuals based on marker genotypes immediately under the LOD peak at chromosome 4. Lengths are adjusted for larval weight. Effect sizes (in blue) for mori:mand and homozugous *B. mandarina* (mand:mand) are the % mean length difference relative to the mori:mori and mori:mand genotypes respectively, normalized by the mean length difference between the parental species.

Figure S4. Analysis of consomic and semi-consomic Chr4 introgression strains.
(A) Schematic diagram showing genome-wide ancestry of semi-consomic (T04) and consomic (CT04) strains. The semiconsomic strain T04 segregates for a *B. mandarina* (Sakado) derived chromosome 4 in an otherwise *B. mori* (p50T) genomic background (69). In contrast, the consomic CT04 strain is

homozygous for the *B. mandarina* (Sakado) derived chromosome 4 in the same *B. mori* (p50T) background. Individual caterpillars were genotyped to identify those with one copy (chr4^{mand}/chr4^{mori}) versus zero copies (chr4^{mori}/chr4^{mori}) of *B. mandarina* chromosome 4 (see Methods). The mean caudal horn length of chr4^{mori}/chr4^{mori} individuals is 15% shorter than chr4^{mand}/chr4^{mori} and chr4^{mand}/chr4^{mand} individuals (**Fig S4**), which is consistent with the direction, dominance and effect size estimated for the chromosome 4 QTL. (B) Caudal horn length distributions among Chr4 genotypes. Caudal horn length was adjusted for larval weight and sex. Effect sizes (in blue) are the % mean length difference relative to the mori:mori genotype, normalized by the mean length difference between the parental species. A significant difference in corrected caudal horn length was observed between mori:mori and mori:mandarina T04 individuals (t-test, $p = 1.0 \times 10^{-8}$; means ± SE: 1.01 ± 0.04 mm vs. 1.44 ± 0.03 mm, respectively).

Figure S5. Caudal horn length is unlikely to have a highly polygenic architecture.
BC1 data shown in panels A, B and C; F2 data shown in panels D, E and F.
(A) The correlation between caudal horn length and genome-wide ancestry for BC1 (Pearson's ρ = 0.32, p= 1.3e-17). Caudal horn length was adjusted for larval weight and sex.
(B) The estimated effect sizes of *B. mandarina* ancestry on each BC_1 chromosome using a model selection approach to select the minimal set of chromosomes that explain caudal horn length. Sex and weight were included as covariates. Bolded chromosomes are chromosomes carrying caudal horn length QTLs.
(C) The correlation between caudal horn length and genome-wide ancestry excluding chromosomes with significant QTLs and Chr3 and Chr6 for BC1 (Pearson's ρ = 0, p= 0.95). Caudal horn length was adjusted for larval weight and sex.
(D) The correlation between caudal horn length and genome-wide ancestry for F2 (Pearson's ρ = 0.45, p= 1.76e-17). Caudal horn length was adjusted for larval weight.
(E) The estimated effect sizes of *B. mandarina* ancestry on each F2 chromosome using a model selection approach to select the minimal set of chromosomes that explain caudal horn length. Sex and weight were included as covariates. Bolded chromosomes are chromosomes carrying caudal horn length QTLs.
(F) The correlation between caudal horn length and genome-wide ancestry excluding chromosomes with significant QTLs and Chr3 and Chr6 for F2 (Pearson's ρ = 0.24, p= 7.7e-6). Caudal horn length was adjusted for larval weight.

Figure S6. Gene expression analysis of parental species and F1 hybrids.
(A) Normalized RNAseq counts from second instar larvae (L2) for non-caudal (A7) and caudal (A8) segments of *B. mori* (Bmori) and *B. mandarina* (Bmand). The asterisk indicates a significant species*segment difference for *Wnt6* (adjusted p-value = 0.023). Numbered genes exclude the prefix "KWMTBOMO", see **Table S3**.
(B) Allele-specific expression of caudal horn (CH) and non-caudal horn (A8) portions of the A8 segment for L1 (first) instar caterpillars (see **Fig 3A**). The fold-difference between *B. mori* (Bmori) and *B. mandarina* (Bmand) alleles is estimated as log2 of the ratio of the averages among the four replicate pools of 10 individuals. Positive values indicate higher expression of the *B. mandarina* allele.
(C) Temporal expression of *Wnt1* and *Wnt6* in the A7 ("non-caudal") segment of *B. mori* and *B. mandarina* throughout fourth instar instar (setting *B. mori* A8 at day 0 of 4th instar = 1). The relative mRNA levels are normalized to that of *ribosomal protein 49* (*rp49*). Error bars represent two standard errors. For caudal segment analysis refer to **Fig 3D**.

Figure S7. Design of CRISPR/Cas9-mediated allele-specific knockouts & breeding and screening strategy
Gene structures and inset alignments of (A) *Wnt1* and (B) *Wnt6* with selected crRNA target sites whose PAM sequences are only present in *B. mandarina*. The target sequences are underlined, and the PAM sequences are shown in bold letters. *B. mandarina* specific SNPs are highlighted with green shadings. Deletions introduced by CRISPR/Cas9 system are indicated by dashes.
(C) Breeding and screening strategy used to generate and phenotype *Wnt* knockouts. T04 individuals (G0) were injected with Cas9-crRNA-tracrRNA complex targeting *Wnt1* or *Wnt6* and crossed to *B. mori* (p50T). G1 progeny were genotyped by heteroduplex mobility assay and Sanger sequenced to identify frameshift mutations. Selected G1 mutants were crossed to *B. mori* to produce G2 larvae. G2s

900 were phenotyped for body weight and caudal horn length, then genotyped using PCR. Because chromosomes other than Chr4 were randomly inherited, off-target effects were assumed to have minimal phenotypic impact. Notably, G2 individuals homozygous for the *B. mori* allele at Chr4 (chr4 mori:mori) did not display aberrant phenotypes.

Fig 1

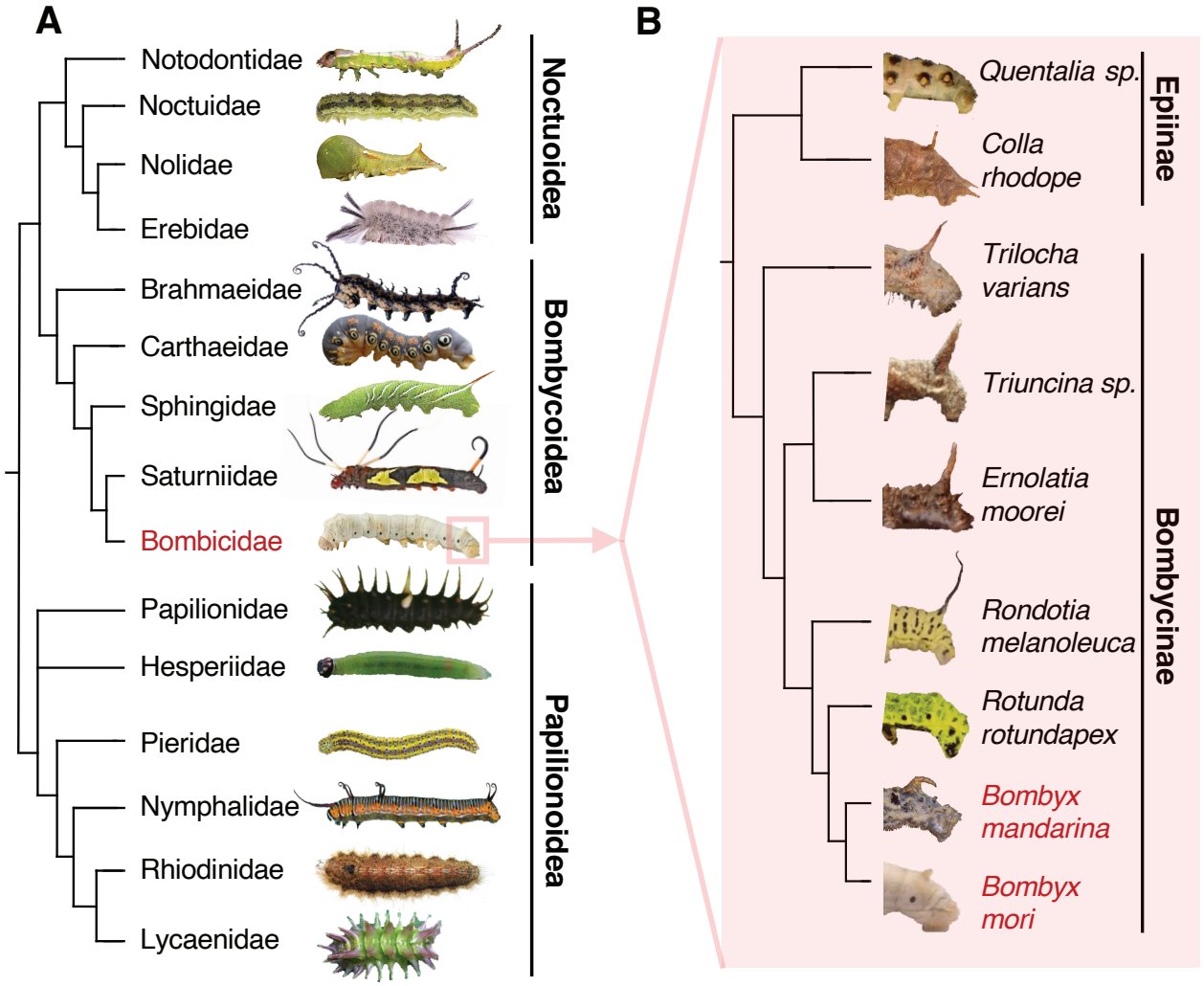

Figure 1. Evolutionary diversification of Lepidopteran larval appendages.

(A) Representative morphological diversity among Lepidopteran caterpillars. Phylogenetic relationships are indicated by the cladogram and family names for each representative species are indicated (based on refs 49-51). Bombyx belongs to the Bombicidae (highlighted in red).

(B) Representative caudal horn diversity among species in the Bombicidae family. Shown are the posterior larval segments for each species; the cladogram depicts their phylogenetic relationships (53-55).

Fig 2

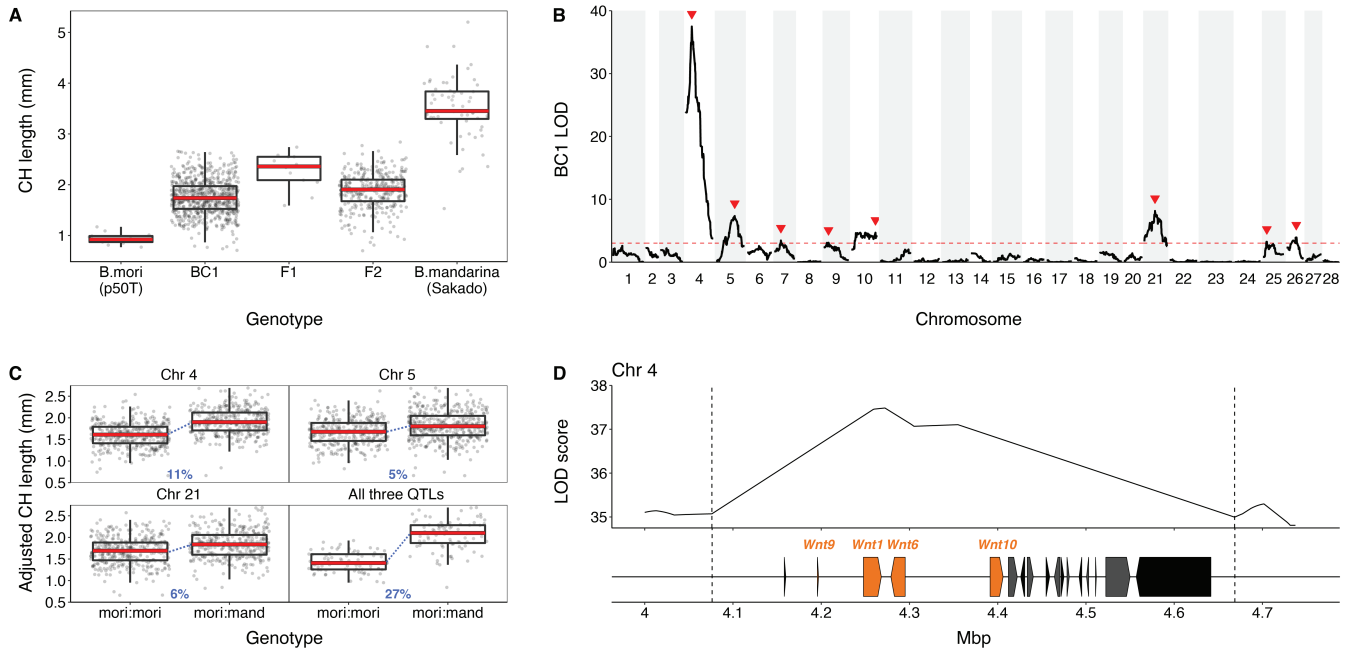

Figure 2. QTL analyses for caudal horn length.
(A) Distributions of caudal horn lengths (CH) in *B. mori* p50T and *B. mandarina* (Sakado) parental species and hybrids. F1 hybrids are the progeny of p50T females × Sakado males; BC1 are the progeny of p50T females and F1 males; F2 are the progeny of F1 hybrids generated by crossing *B. mori* p50T males and *B. mandarina* Sakado females.
(B) QTL LOD profile plots for caudal horn length based on the BC1 mapping panel. LOD is shown in black with a red dashed line indicating the estimated significance threshold (3.02) determined by 1000 phenotype permutations. Red arrows indicate significant QTL peaks.
(C) Caudal horn length distributions of BC1 individuals based on marker genotypes immediately under the three highest LOD peaks on chromosomes 4, 5, and 21. Caudal horn lengths are adjusted for larval weight and sex. The last panel shows caudal horn distributions of BC1 individuals whose genotypes are jointly homozygous *B. mori* or jointly heterozygous at all three QTL. The % mean length difference between mori:mori and mori:mand genotypes normalized by the mean length difference between the parental species for each peak are noted in blue.
(D) Annotation of the chromosome 4 QTL interval. Boxes indicate annotated genes within the 1.5 LOD interval (delimited by dashed lines) estimated in the BC1 QTL analysis (**Table S3**). *Wnt*-family genes are colored in orange. Coordinates are in Mega base pairs (Mbp).

Fig 3

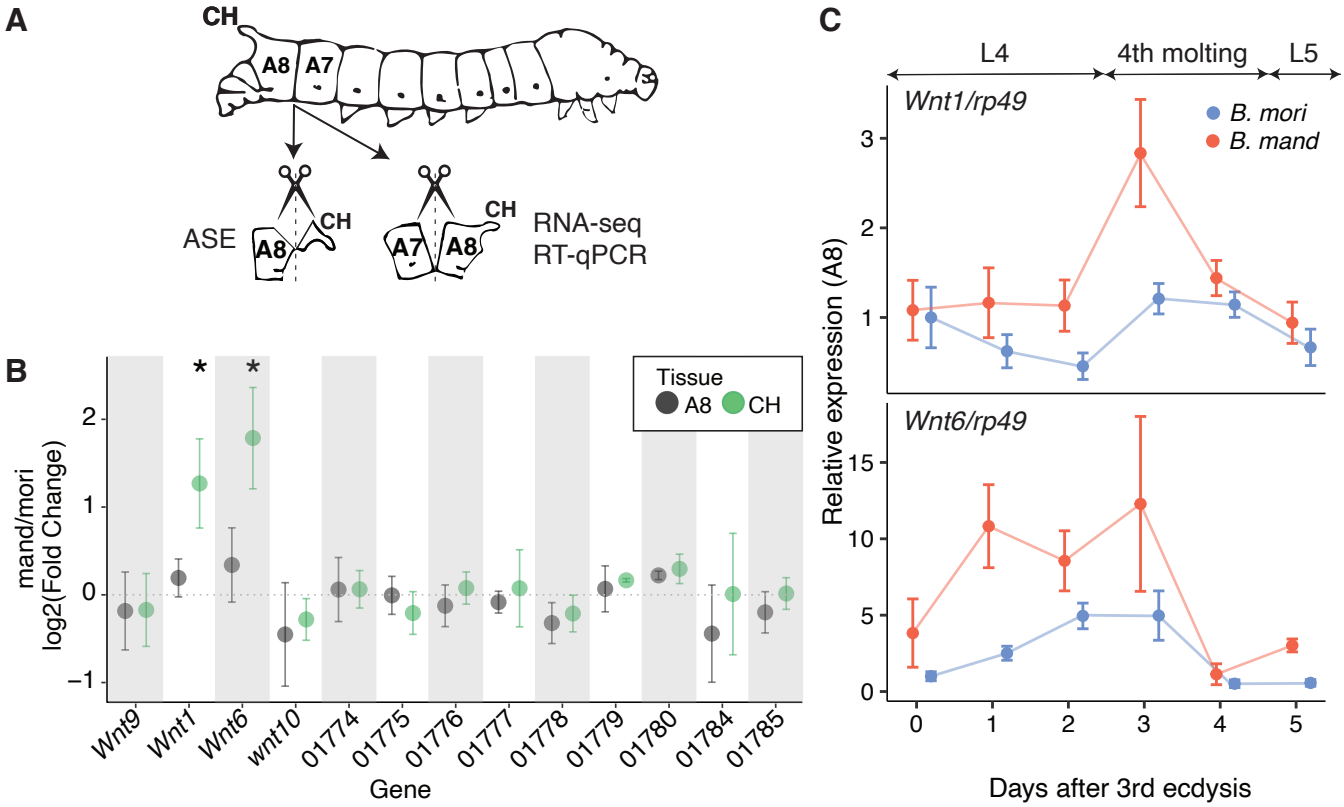

Figure 3. Cis-regulatory divergence underlies species- and tissue-specific *Wnt1* and *Wnt6* expression patterns during larval development.

(A) Schematic of the sampling scheme for gene expression analyses. Total RNA was extracted from caudal horn (CH, segment A8) and non-horn tissue of the eighth abdominal segment (A8) for RNA-seq (**Fig S6A**) and targeted ASE (**Fig 3B and Fig S6B**). Total RNA from the integument of segments A7 and A8 was extracted for RNA-seq (**Fig S6A**) and the temporal expression analysis (**Fig 3C and Fig S6C**).

(B) Allele-specific expression patterns in the caudal horn of *B. mori* (p50T) × *B. mandarina* (Sakado) F1 hybrids of L5 (final) instar caterpillars. Plotted for each gene in the QTL interval (in the same order, left to right), is the log2(fold-difference) in the average *B. mori* and *B. mandarina* allele counts for the caudal horn portion of segment A8. Values larger than 0 indicate higher expression of the *B. mandarina* allele and whiskers represent two standard errors (corresponding to 95% confidence intervals among biological replicates). "CH" shows the caudal horn tissue and "A8" the non-horn tissue portion (Fig3A). A corresponding analysis of L1 (first) instar caterpillars is shown in **Fig S6B**. Significance of ASE differences between the caudal and non-caudal portions of segment A8 were evaluated using the inverted beta-binomial test (ibb) test for paired count data and significant differences are indicated with asterisks (Bonferroni corrected, **Table S5**).

(C) Temporally-elevated expression of *Wnt1* and *Wnt6* in segment A8 of *B. mandarina*. Temporal expression of *Wnt1* and *Wnt6* in the integument tissue of segment A8 during the transition between fourth and fifth instar stages of *B. mori* and *B. mandarina* caterpillar development. A corresponding analysis of segment A7 is shown in **Fig. S6C**. Relative *Wnt1* and *Wnt6* expression levels (setting *B. mori* A8 at day 0 of 4th instar = 1) were normalized to those of *ribosomal protein 49* (*rp49*). Whiskers represent two standard errors among replicates.

Fig 4

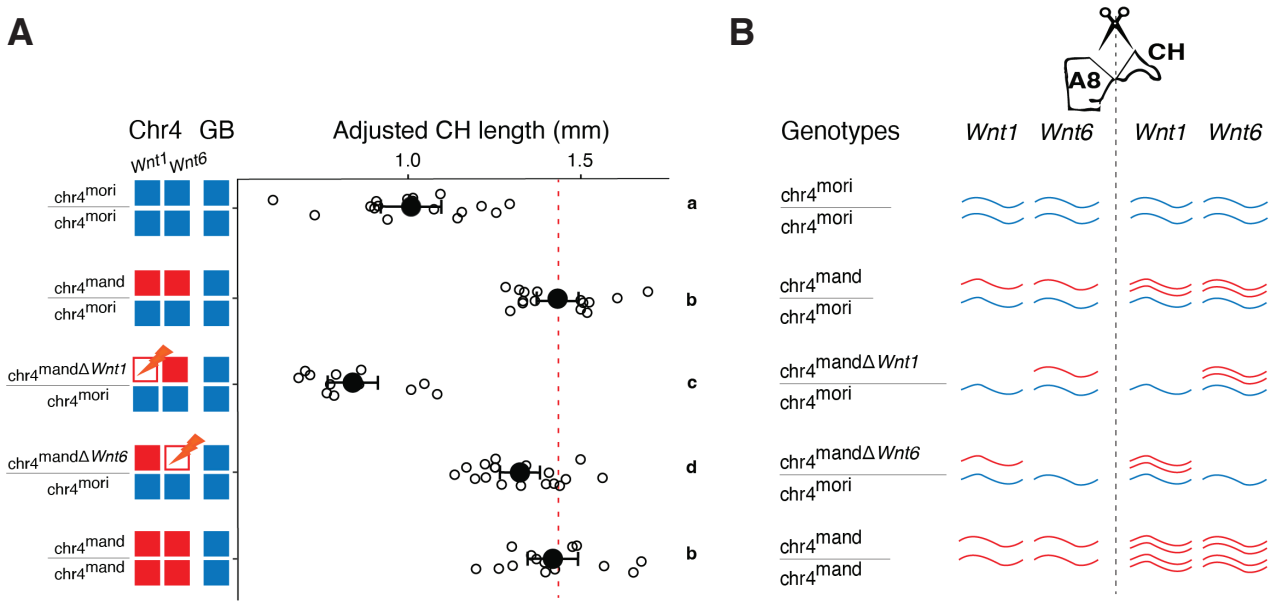

Figure 4. *Wnt1* and *Wnt6* CRISPR/Cas9-mediated *B. mandarina*-allele-specific knockouts significantly reduce caudal horn length.

(A) Distributions of caudal horn lengths for larvae at day 0 of the fifth instar (L5). Diagrams to the left indicate the genotypes of the strains being compared (Chr4=chromosome 4; GB=genomic background). Blue corresponds to the p50T *B. mori* background; and red to the *B. mandarina* Sakado background. $chr4^{mand\Delta Wnt1}/chr4^{mori}$ and $chr4^{mand\ Wnt6}/chr4^{mori}$ correspond to CRISPR/Cas9-mediated *B. mandarina*-allele-specific knockouts of *Wnt1* and *Wnt6*, respectively. White points indicate individual caterpillar horn lengths, corrected for caterpillar weight (a proxy for size). Black points and whiskers correspond to means and standard errors. Letters on the right indicate groups that differ significantly in caudal horn length based on a one-way ANOVA followed by Tukey's HSD test (family-wise confidence level = 95%). A significant positive allometric relationship was observed between body weight and caudal horn length (ANCOVA: effect of weight, $p = 2.9 \times 10^{-16}$), with a significantly steeper slope in *B. mandarina* than in *B. mori* (interaction term, $p = 0.016$), see **Fig S1**.

(B) Conceptual representation of relative *Wnt1* and *Wnt6* transcriptional abundances for each genotype. Expression results (**Fig 3**) indicate that *Wnt1* and *Wnt6* have elevated transcript abundance in caudal horn tissue of stage L5 *B. mandarina* caterpillars. Knock-outs of the *B. mandarina* allele are expected to decrease (but not eliminate) expression of *Wnt1* or *Wnt6* relative to all other genotypes in the entire animal.

Fig S1

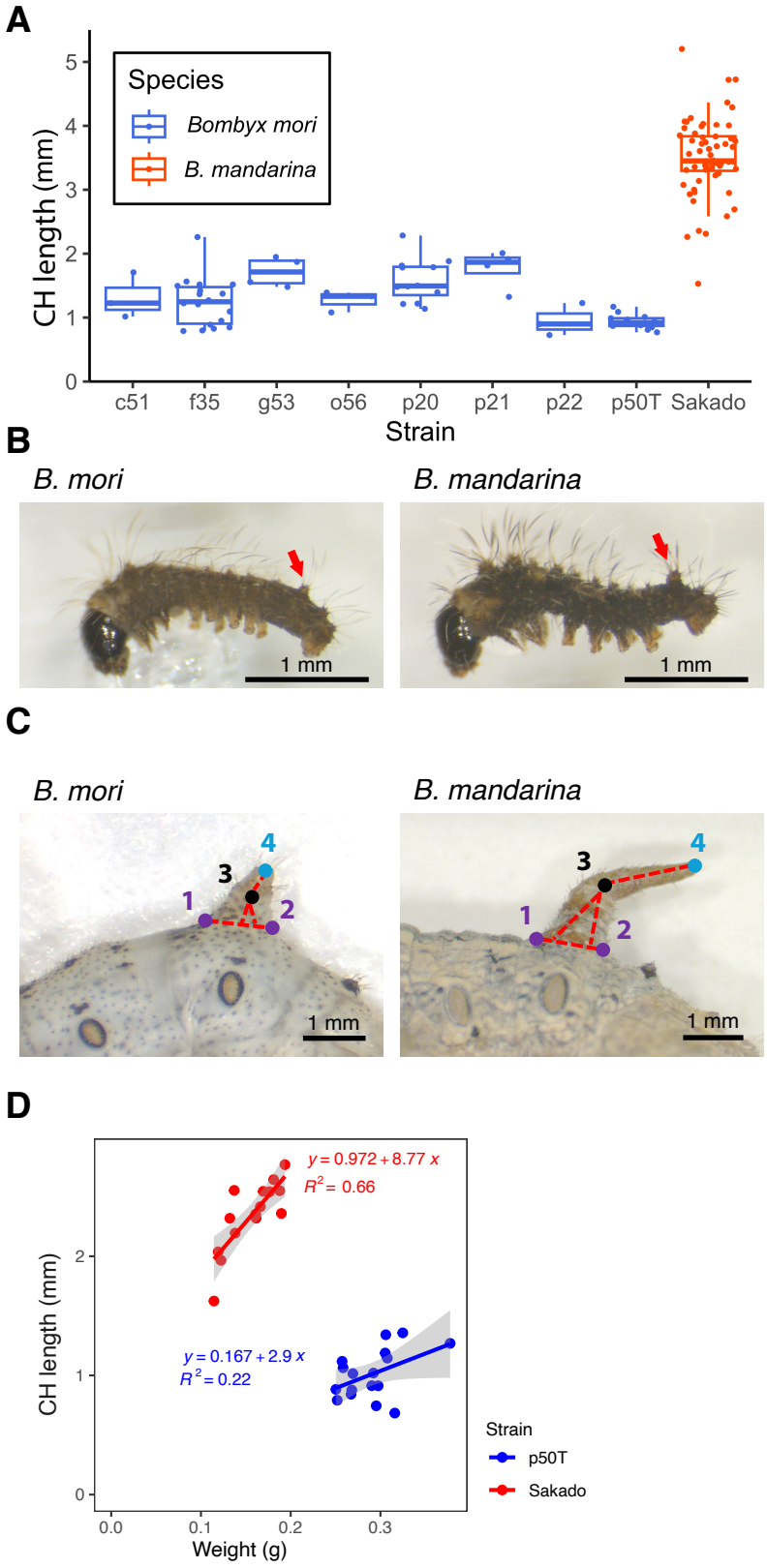
A
Species
Bombyx mori
B. mandarina
CH length (mm)
0
1
2
3
4
5
c51
f35
g53
o56
p20
p21
p22
p50T
Sakado
Strain
B
B. mori
B. mandarina
1 mm
1 mm
C
B. mori
B. mandarina
1
2
3
4
1 mm
1 mm
D
y = 0.972 + 8.77 x
R2 = 0.66
y = 0.167 + 2.9 x
R2 = 0.22
CH length (mm)
0
1
2
0.0
0.1
0.2
0.3
Weight (g)
Strain
p50T
Sakado

Fig S1 (cont)

Figure S1. Measurement of caudal horn length variation.
(A) Caudal horn (CH) length measurements across various strains of *B. mori* and *B. mandarina* Sakado. The *B. mori* strain used in this study is p50T. Values were not adjusted for weight or sex.
(B) Neonate (day 0 of first instar) larvae of *B. mori* (left) and *B. mandarina* (right). Red arrows indicate the caudal horns. Scale bars = 1 mm.
(C) Measuring the caudal horn. Images of L5 larval caudal horns were marked at three locations (colored points) using MATLAB or ImageJ. Two purple points are laid to mark the base of the caudal horn, corresponding to $X_{1,2}$,$Y_{1,2}$ (see Methods: Rearing and Phenotyping), and the black point marks the vertex X_3,Y_3. The height of the triangle is then added to the distance between the black point and the blue point X_4,Y_4 located at the tip of the caudal horn.
(D) Caudal horn (CH) length and caterpillar weight relationship for *B. mori* (p50T) and *B. mandarina* (Sakado) at L5 stage. Values were not adjusted for weight or sex.

Fig S2

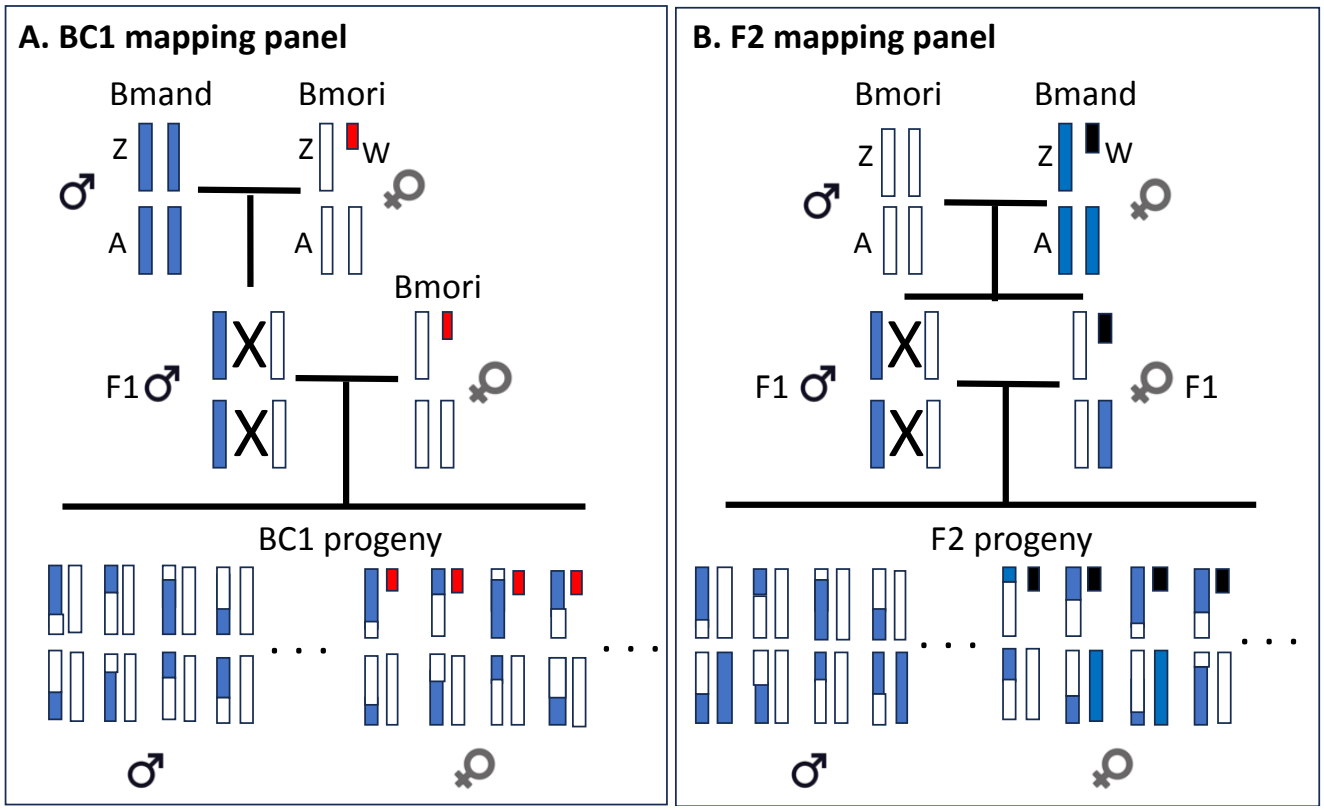

Figure S2. Schematic of the cross design for the BC1 and F2 mapping panels.
(A) The BC1 mapping panel. *B. mandarina* Sakado (Bmand) males were crossed to *B. mori* (Bmori) p50T females to create F1 males. F1 males were then backcrossed to *B. mori* p50T to produce BC1 progeny. Note that the W chromosome of BC1 females (red) is derived from *B. mori* p50T. The large X indicates meiotic crossing over in F1 males.
(B) The F2 mapping panel. *B. mori* p50T (Bmori) males were crossed to a *B. mandarina* (Bmand) Sakado females to create F1 males. F1 males and females were crossed to produce F2 progeny. Note that the W chromosome of F2 females (black) is derived from *B. mandarina* Sakado. The large X indicates meiotic crossing over in F1 males.

Fig S3

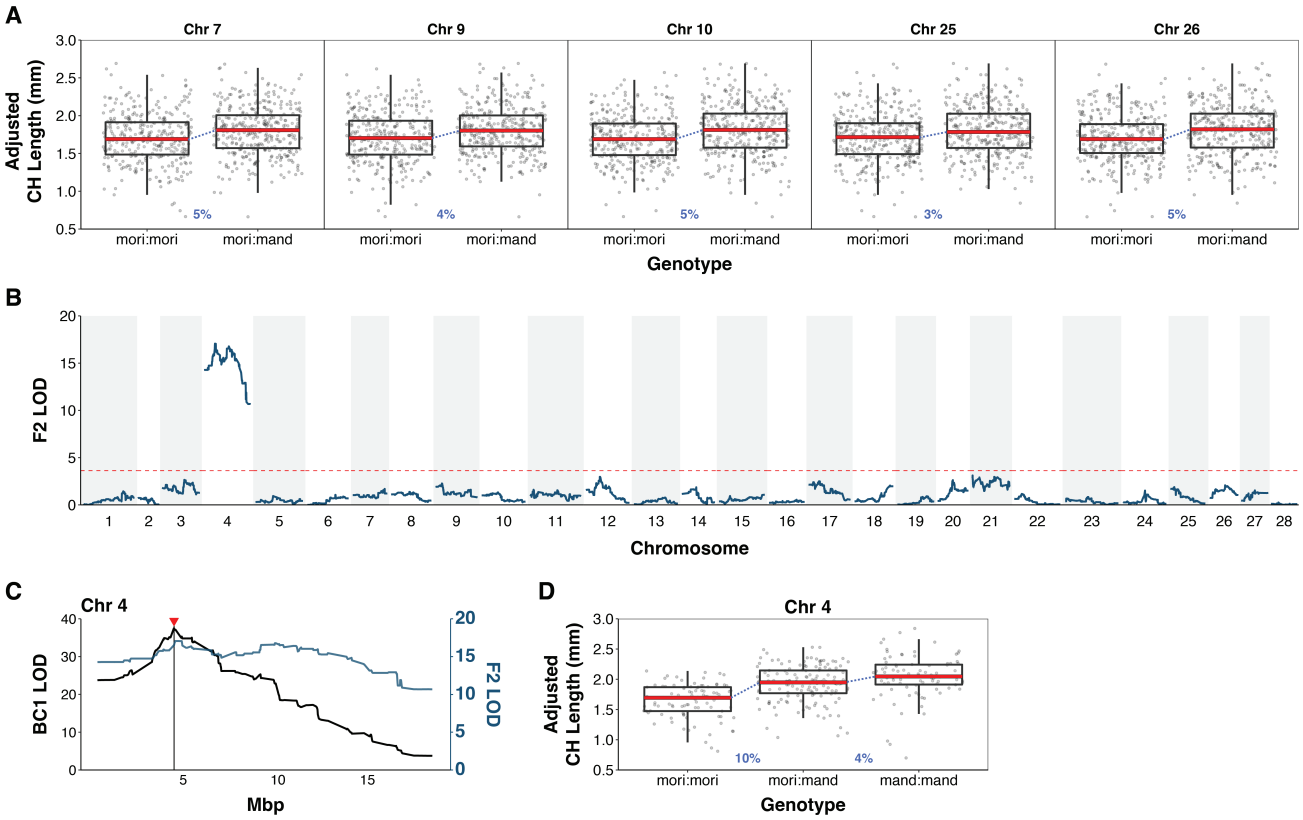

Figure S3. F2 QTL analysis and estimated QTL effect sizes.
(A) Caudal horn (CH) length distributions of BC1 individuals based for markers corresponding to maximum LOD peaks for QTLs on chromosomes 7, 9, 10, 25, and 26. Caudal horn length was adjusted for larval sex and weight. Effect sizes (in blue) are the % mean length difference between heterozygous (mori:mand) and homozugous *B. mori* (mori:mori) genotype, normalized by the mean length difference between the parental species.
(B) F2 QTL LOD profile for caudal horn length. LOD is shown in blue with the red dashed line indicating the LOD significance threshold of 3.62 determined by 1000 permutations.
(C) Superposition of BC1 (black) and F2 (blue) LOD profiles for Chr4. The vertical line and red triangle indicate the max LOD position in BC1. LOD significance threshold for BC1 is 3.02, and F2 is 3.62.
(D) Caudal horn length distributions of F2 individuals based on marker genotypes immediately under the LOD peak at chromosome 4. Lengths are adjusted for larval weight. Effect sizes (in blue) for mori:mand and homozugous *B. mandarina* (mand:mand) are the % mean length difference relative to the mori:mori and mori:mand genotypes respectively, normalized by the mean length difference between the parental species.

Fig S4

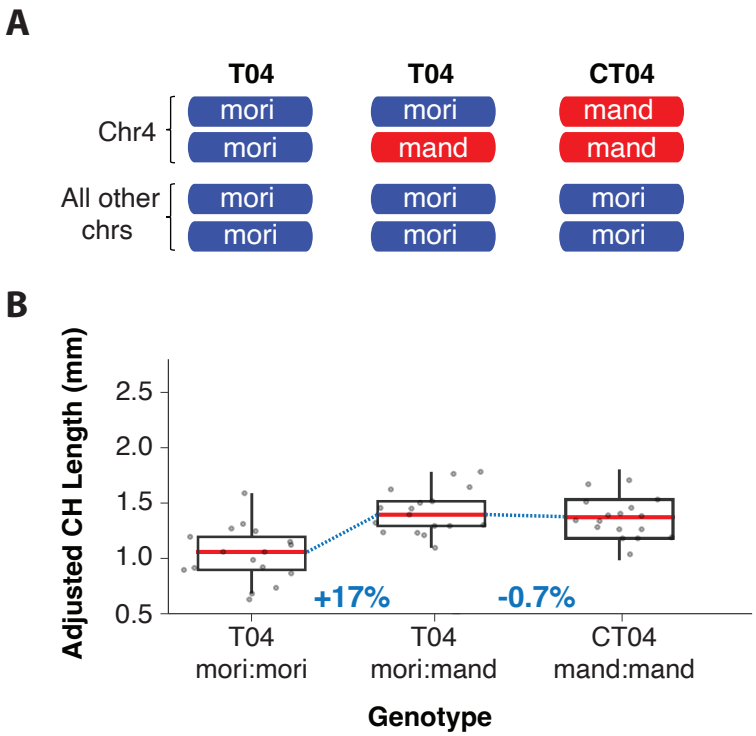

Figure S4. Analysis of consomic and semi-consomic Chr4 introgression strains.
(A) Schematic diagram showing genome-wide ancestry of semi-consomic (T04) and consomic (CT04) strains. The semiconsomic strain T04 segregates for a *B. mandarina* (Sakado) derived chromosome 4 in an otherwise *B. mori* (p50T) genomic background (24). In contrast, the consomic CT04 strain is homozygous for the *B. mandarina* (Sakado) derived chromosome 4 in the same *B. mori* (p50T) background. Individual caterpillars were genotyped to identify those with one copy ($chr4^{mand}/chr4^{mori}$) versus zero copies ($chr4^{mori}/chr4^{mori}$) of *B. mandarina* chromosome 4 (see Methods). The mean caudal horn length of $chr4^{mori}/chr4^{mori}$ individuals is 15% shorter than $chr4^{mand}/chr4^{mori}$ and $chr4^{mand}/chr4^{mand}$ individuals (**Fig S4**), which is consistent with the direction, dominance and effect size estimated for the chromosome 4 QTL. (B) Caudal horn length distributions among Chr4 genotypes. Caudal horn length was adjusted for larval weight and sex. Effect sizes (in blue) are the % mean length difference relative to the mori:mori genotype, normalized by the mean length difference between the parental species. A significant difference in corrected caudal horn length was observed between mori:mori and mori:mandarina T04 individuals (t-test, $p = 1.0 \times 10^{-8}$; means ± SE: 1.01 ± 0.04 mm vs. 1.44 ± 0.03 mm, respectively).

Fig S5

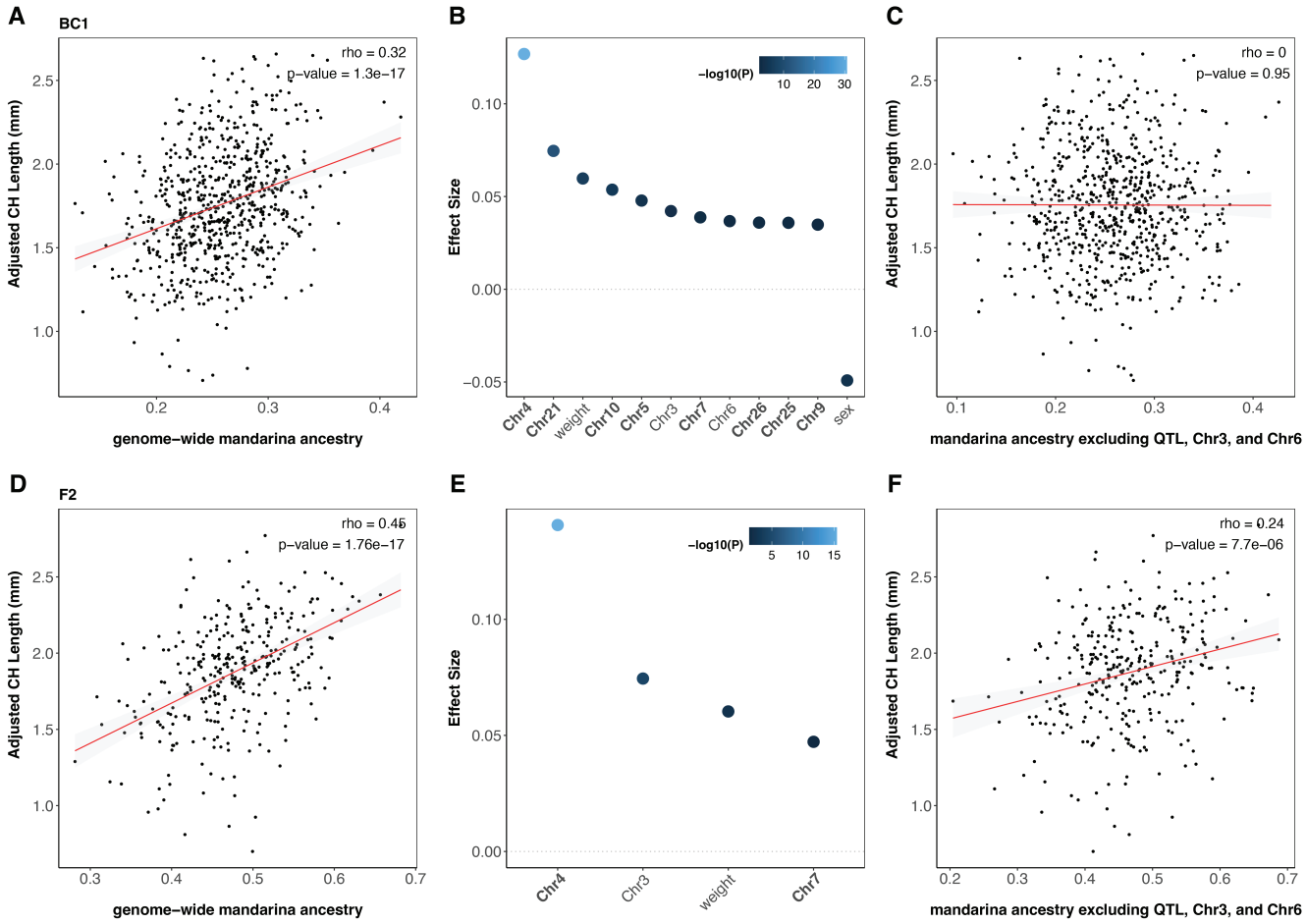

Figure S5. Caudal horn length is unlikely to have a highly polygenic architecture.
BC1 data shown in panels A, B and C; F2 data shown in panels D, E and F.

(A) The correlation between caudal horn length and genome-wide ancestry for BC1 (Pearson's ϱ = 0.32, p= 1.3e-17). Caudal horn length was adjusted for larval weight and sex.

(B) The estimated effect sizes of *B. mandarina* ancestry on each BC_1 chromosome using a model selection approach to select the minimal set of chromosomes that explain caudal horn length. Sex and weight were included as covariates. Bolded chromosomes are chromosomes carrying caudal horn length QTLs.

(C) The correlation between caudal horn length and genome-wide ancestry excluding chromosomes with significant QTLs and Chr3 and Chr6 for BC1 (Pearson's ϱ = 0, p= 0.95). Caudal horn length was adjusted for larval weight and sex.

(D) The correlation between caudal horn length and genome-wide ancestry for F2 (Pearson's ϱ = 0.45, p= 1.76e-17). Caudal horn length was adjusted for larval weight.

(E) The estimated effect sizes of *B. mandarina* ancestry on each F2 chromosome using a model selection approach to select the minimal set of chromosomes that explain caudal horn length. Sex and weight were included as covariates. Bolded chromosomes are chromosomes carrying caudal horn length QTLs.

(F) The correlation between caudal horn length and genome-wide ancestry excluding chromosomes with significant QTLs and Chr3 and Chr6 for F2 (Pearson's ϱ = 0.24, p= 7.7e-6). Caudal horn length was adjusted for larval weight.

Fig S6

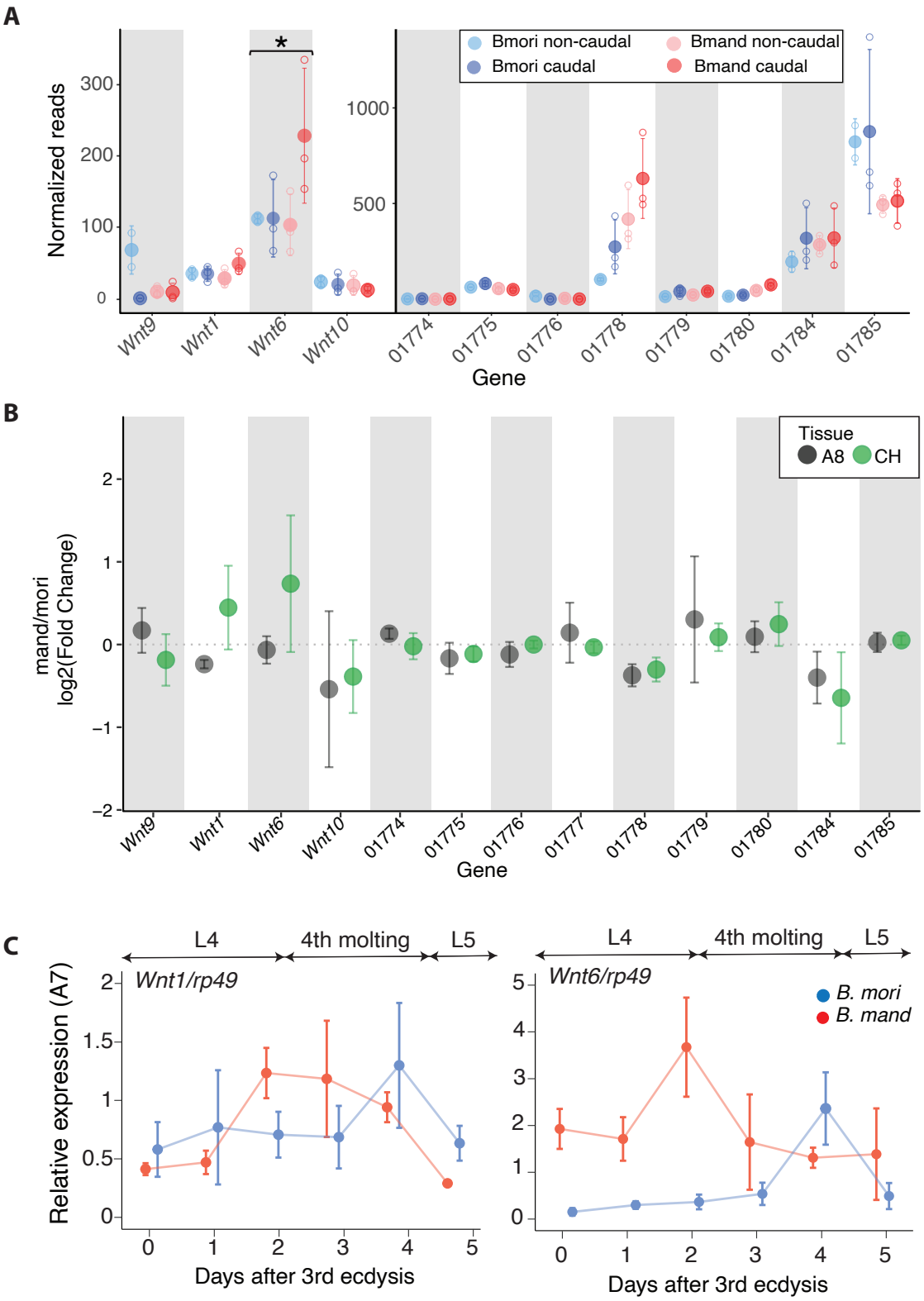
A
Normalized reads
Bmori non-caudal
Bmori caudal
Bmand non-caudal
Bmand caudal
*
Wnt9
Wnt1
Wnt6
Wnt10
01774
01775
01776
01778
01779
01780
01784
01785
Gene
B
mand/mori
log2(Fold Change)
Tissue
A8
CH
Wnt9
Wnt1
Wnt6
Wnt10
01774
01775
01776
01777
01778
01779
01780
01784
01785
Gene
C
L4
4th molting
L5
Wnt1/rp49
Relative expression (A7)
Days after 3rd ecdysis
Wnt6/rp49
B. mori
B. mand
Days after 3rd ecdysis

Fig S6 (cont)

Figure S6. Gene expression analysis of parental species and F1 hybrids.
(A) Normalized RNAseq counts from second instar larvae (L2) for non-caudal (A7) and caudal (A8) segments of *B. mori* (Bmori) and *B. mandarina* (Bmand). The asterisk indicates a significant species*segment difference for *Wnt6* (adjusted p-value = 0.023). Numbered genes exclude the prefix "KWMTBOMO", see **Table S3**.
(B) Allele-specific expression of caudal horn (CH) and non-caudal horn (A8) portions of the A8 segment for L1 (first) instar caterpillars (see **Fig 3A**). The fold-difference between *B. mori* (Bmori) and *B. mandarina* (Bmand) alleles is estimated as log2 of the ratio of the averages among the four replicate pools of 10 individuals. Positive values indicate higher expression of the *B. mandarina* allele.
(C) Temporal expression of *Wnt1* and *Wnt6* in the A7 ("non-caudal") segment of *B. mori* and *B. mandarina* throughout fourth instar instar (setting *B. mori* A8 at day 0 of 4th instar = 1). The relative mRNA levels are normalized to that of *ribosomal protein 49* (*rp49*). Error bars represent two standard errors. For caudal segment analysis refer to **Fig 3D**.

Fig S7

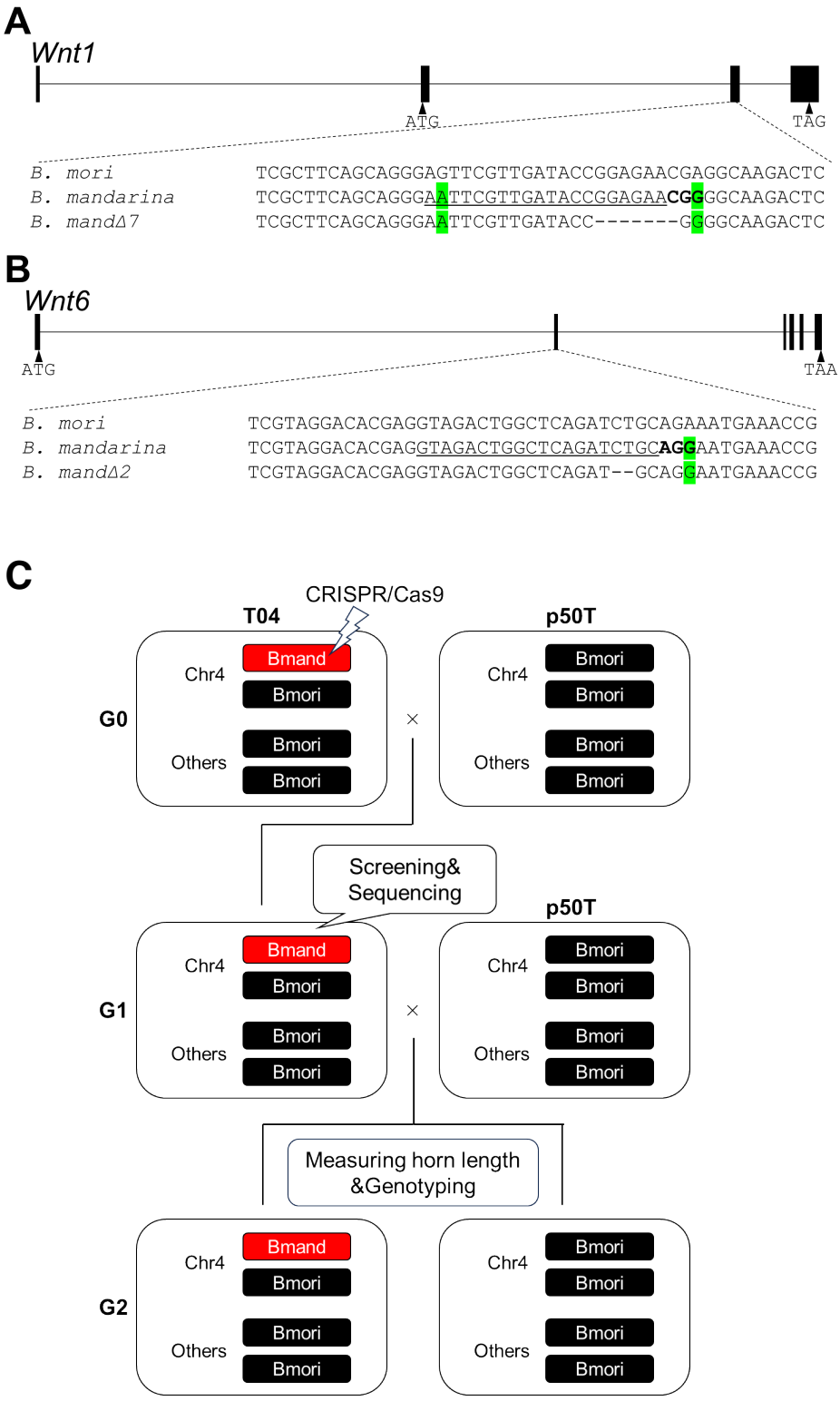
A
Wnt1
ATG
TAG
B. mori TCGCTTCAGCAGGGAGTTCGTTGATACCGGAGAACGAGGCAAGACTC
B. mandarina TCGCTTCAGCAGGGAATTCGTTGATACCGGAGAACGGGGCAAGACTC
B. mandΔ7 TCGCTTCAGCAGGGAATTCGTTGATACC-------GGGGCAAGACTC
B
Wnt6
ATG
TAA
B. mori TCGTAGGACACGAGGTAGACTGGCTCAGATCTGCAGAAATGAAACCG
B. mandarina TCGTAGGACACGAGGTAGACTGGCTCAGATCTGCAGGAATGAAACCG
B. mandΔ2 TCGTAGGACACGAGGTAGACTGGCTCAGAT--GCAGGAATGAAACCG
C
CRISPR/Cas9
T04
p50T
G0
Chr4
Bmand
Bmori
Others
Bmori
Bmori
×
Screening&
Sequencing
G1
G2
Measuring horn length
&Genotyping

Fig S7 (cont)

Figure S7. Design of CRISPR/Cas9-mediated allele-specific knockouts & breeding and screening strategy

Gene structures and inset alignments of (A) *Wnt1* and (B) *Wnt6* with selected crRNA target sites whose PAM sequences are only present in *B. mandarina*. The target sequences are underlined, and the PAM sequences are shown in bold letters. *B. mandarina* specific SNPs are highlighted with green shadings. Deletions introduced by CRISPR/Cas9 system are indicated by dashes.

(C) Breeding and screening strategy used to generate and phenotype *Wnt* knockouts. T04 individuals (G0) were injected with Cas9-crRNA-tracrRNA complex targeting *Wnt1* or *Wnt6* and crossed to *B. mori* (p50T). G1 progeny were genotyped by heteroduplex mobility assay and Sanger sequenced to identify frameshift mutations. Selected G1 mutants were crossed to *B. mori* to produce G2 larvae. G2s were phenotyped for body weight and caudal horn length, then genotyped using PCR. Because chromosomes other than Chr4 were randomly inherited, off-target effects were assumed to have minimal phenotypic impact. Notably, G2 individuals homozygous for the *B. mori* allele at Chr4 (chr4 mori:mori) did not display aberrant phenotypes.